catalysts

MDPI

Review

Atomically Dispersed Catalytic Sites: A New Frontier for Cocatalyst/Photocatalyst Composites toward Sustainable Fuel and Chemical Production

Shuping Zhang, Bing Bai, Jia Liu * and Jiatao Zhang *

Beijing Key Laboratory of Construction-Tailorable Advanced Functional Materials and Green Applications, Beijing Institute of Technology, School of Materials Science & Engineering, Beijing 100081, China; Zhangshuping1048@163.com (S.Z.); Baibinghardwork@163.com (B.B.)
* Correspondence: liujia86@bit.edu.cn (J.L.); zhangjt@bit.edu.cn (J.Z.)

Abstract: Photocatalysis delivers a promising pathway toward the clean and sustainable energy supply of the future. However, the inefficiency of photon absorption, rapid recombination of photogenerated electron-hole pairs, and especially the limited active sites for catalytic reactions result in unsatisfactory performances of the photocatalytic materials. Single-atom photocatalysts (SAPCs), in which metal atoms are individually isolated and stably anchored on support materials, allow for maximum atom utilization and possess distinct photocatalytic properties due to the unique geometric and electronic features of the unsaturated catalytic sites. Very recently, constructing SAPCs has emerged as a new avenue for promoting the efficiency of sustainable production of fuels and chemicals via photocatalysis. In this review, we summarize the recent development of SAPCs as a new frontier for cocatalyst/photocatalyst composites in photocatalytic water splitting. This begins with an introduction on the typical structures of SAPCs, followed by a detailed discussion on the synthetic strategies that are applicable to SAPCs. Thereafter, the promising applications of SAPCs to boost photocatalytic water splitting are outlined. Finally, the challenges and prospects for the future development of SAPCs are summarized.

Keywords: single atom; cocatalyst; photocatalytic water splitting; hydrogen generation

Citation: Zhang, S.; Bai, B.; Liu, J.; Zhang, J. Atomically Dispersed Catalytic Sites: A New Frontier for Cocatalyst/Photocatalyst Composites toward Sustainable Fuel and Chemical Production. *Catalysts* **2021**, *11*, 1168. https://doi.org/10.3390/catal11101168

Academic Editor: Petr Praus

Received: 25 July 2021
Accepted: 25 September 2021
Published: 27 September 2021

1. Introduction

Since the pioneering discovery of water photolysis on TiO_2 electrodes in 1972, solar-driven water splitting has been recognized as one of the most promising ways to transform solar energy into renewable and clean hydrogen energy [1]. The photocatalysts are the key component of photocatalytic processes [2]. Over the past few decades, researchers have developed various photocatalysts toward the application of water splitting [3–5]. A typical photocatalytic water splitting reaction on semiconductor photocatalysts mainly involves three primary steps: (1) absorption of light to generate electron-hole pairs; (2) separation of the photogenerated electron-hole pairs and their migration to semiconductor surfaces; and (3) consumption of the photogenerated electrons and holes via surface redox reactions. Specifically, only the photogenerated electrons and holes that successfully reach the surface of the catalyst have the possibility to react with water. Therein, the water molecules can be reduced by photogenerated electrons to generate H_2 (hydrogen evolution reaction, HER), and at the same time oxidized by photogenerated holes to generate oxygen (Oxygen evolution reaction, OER), hydrogen peroxide, superoxide radicals, etc. [6]. The problem is that the single-component photocatalyst always suffers from poor photocatalytic activities because of its narrow light harvesting range, serious electron-hole recombination, and weak adsorption and activation abilities for reactant molecules. To overcome these bottlenecks, strategies aiming to expand the light absorption range, construct interface heterojunctions, and engineer surface reaction sites by rational design of multicomponent photocatalysts

have been developed [7,8]. Among these, the loading of a cocatalyst is an effective method to improve the functions of a photocatalyst [9]. For example, noble metals, such as Pt and Pd nanoparticles, are considered as efficient cocatalysts for promoting photocatalytic H_2 evolution [10]. However, the high cost of these noble metal particles strongly hinders their wide utilization.

Single-atom photocatalysts (SAPCs) with maximized atomic utilization can effectively improve the number of exposed reaction sites on surface while reducing the loading amount of the noble metal cocatalyst [11,12]. For SAPCs, the atomically dispersed metal atoms could be anchored on the support materials by forming coordination with the host atoms, which helps to prevent agglomeration of the monodispersed metal atoms with high surface energy [13]. Compared with metal nanoparticles, the coordination interaction with the support atoms makes the single metal atoms possess a unique local electronic and geometric structure [14]. In addition, the electron transfer and charge redistribution between the single metal atoms and supports may reduce the reaction barriers to enhancing catalytic performance [15]. Nevertheless, due to the high surface free energy of isolated atoms, their aggregation is always unavoidable, and this is significantly detrimental to photocatalytic activity and stability. Therefore, how to develop SAPCs with high activity, selectivity, and stability, and how to unravel the structure-activity relationship of SAPCs still remain as the research focus in this area. In this review, the recent advances in exploiting SAPCs as the new prototype of cocatalyst/photocatalyst composites toward water splitting are introduced, especially from the aspect of their atomic structure, synthetic strategy, and applications. Then, the challenges and future research directions of single-atom photocatalysts are discussed.

2. Structure of SAPCs

Generally, SAPCs are composed of support materials and monodispersed cocatalyst atoms. In this system, the support materials provide stable anchors for the spatially isolated single metal atoms to restrict their migration, while the single metal atoms act as active reaction centers to boost the surface reaction. Especially for photocatalytic applications, the support materials often constituted by semiconductors are also responsible for the generation and separation of electron and hole carriers, which need to transfer to semiconductor surface to reach the reaction sites [16]. The photocatalytic performance of SAPCs strongly relies on the support, the single-atom cocatalyst, as well as the interaction between them [17]. Synergistic manipulation is highly desirable to make the SAPCs show distinct and excellent performance in photocatalytic water splitting reactions.

2.1. Support Materials

The support used to host single atoms should provide enough surface sites to establish stable anchoring and coordination for singe metal atoms, capable of circumventing their aggregation caused by the high surface free energy [18]. Regarding photocatalytic applications, materials with a high specific surface area, appropriate coordinated atoms, good optical absorption, and fast charge carrier transportation capability are the ideal supports [19,20]. Generally, the supports of SAPCs are inorganic or organic semiconductor materials (or materials with semiconductor properties) such as metal oxide, metal sulfide, graphite-like carbon nitride (g-C_3N_4), metal organic framework (MOF), covalent organic framework (COF), partially oxidized graphene (GO), nitrogen-doped graphene (NG), etc., as well as metals with a unique localized surface plasmon resonance (LSPR) effect. In addition, when combined with suitable light-absorbing materials, carbon-based materials with excellent conductivity have also been widely used as supports for photocatalytic SAPCs [21].

2.1.1. Inorganic Materials

Metal oxides, metal sulfides, and other inorganic semiconductor materials with appropriate bandgaps such as TiO_2, ZnO, WO_3, ZrO_2, CdS, GaS, MoS_2, $BiVO_3$, BiOX (x = Cl, Br), $SrTiO_3$, etc. have been frequently used as photocatalysts [22–26]. The abundant coordination atoms of O, S in the lattice and surface of these materials can provide a strong anchoring effect for stabilizing the single metal atoms.

For metal oxide supports, individual metal atoms can be firmly anchored by forming chemical bonds with O atoms or superseding the sites of cations in supports [27,28]. TiO_2 is the earliest discovered photocatalytic active materials and possesses the merits of low price, good thermal and photochemical stability, and nontoxicity [29,30]. TiO_2 supports used in SAPCs usually are two-dimensional nanosheets [31], or have nanoporous [32,33] or mesoporous structures [34], which all possess a large specific surface area and expose abundant active sites. The bandgap of TiO_2 can be changed by morphology tuning. Batzill et al. reported that the bandgap of TiO_2 was narrowed from 3.2 eV for bulk TiO_2 to 2.1 eV for TiO_2 nanosheet, which closely matches the energy range of visible light [35]. Ishihara et al. [36] prepared an Rh-doped TiO_2 nanosheet (Figure 1a). According to the results of high-angle annular dark-field scanning transmission electron microscopy (HAADF-STEM) and extended X-ray absorption fine structure (EXAFS) (Figure 1b–e), the isolated single-atom Rh dopants substitute Ti^{4+} in two-dimensional TiO_2 crystals. The single Rh atom in crystal acted as an efficient reaction center in photocatalytic water splitting process and significantly improved the photocatalytic H_2 evolution activity. The photocatalytic activity for HER on this single-atom Rh-doped nanosheet was 10 times higher than that of undoped nanosheet. In addition, by controlling the morphology of TiO_2, the exposed crystal planes can be changed to obtain different geometry and electronic structure [37]. Liu et al. successfully synthesized single-atom Pt on nanosized TiO_2 single crystals with highly exposed (001) facets (TiO_2-A) through photo-deposition method [22]. In their study, the atomically dispersed Pt atoms were selectively dispersed on the (101) facets of TiO_2-A while Pt nanoparticles were formed on commercial anatase nanoparticles (TiO_2-0) under the same synthesized condition (As shown in Figure 1f). The isolated Pt atoms increased the number of photocatalytic active sites and inhibited the recombination of photogenerated electrons and holes. The Pt_1/TiO_2-A displayed significantly higher photocatalytic activity (0.6Pt/TiO_2-A, 84.5 umol/h) as well as considerable stability for H_2 evolution compared to Pt/TiO_2 -0 (0.6Pt/TiO_2-0, 18.8 umol/h) (Figure 1g).

Metal sulfides, such as CdS, MoS_2, GaS, and so on, with smaller bandgaps compared to metal oxides, have also been widely used as supports for SAPCs [19,38–40]. The abundant S atoms in metal sulfides can provide strong coordination with single atoms [41]. Zhang et al. decorated the surface step edges of CdS nanowires (NWs) with isolated Pt atoms to promote photocatalytic HER (Figure 2a,b) [42]. According to EXAFS curve fitting results, the isolated Pt atoms were strongly anchored on CdS surface by bonding with four unsaturated S atoms (Figure 2c). As such, the utilization efficiency of noble Pt co-catalysts was significantly increased. Moreover, the HER activity of single Pt atom decorated-CdS NWs was greatly enhanced, which was 7.69 and 63.77 times higher than that of Pt nanoparticles decorated-CdS NWs and bare CdS NWs, respectively. Besides S atoms, the surface hydroxyl groups bonded to metal sulfide can also serve as anchoring sites. Zhong et al. reported an catalyst composed of atomically dispersed Ni on CdS nanorods (denoted as Ni_1/CdS NRs, Figure 2d) prepared by a simple photochemical method [43]. X-ray absorption near edge structure (XANES) spectra indicated that the chemical state of Ni in Ni_1/CdS NRs was similar to $Ni(OH)_2$ (Figure 2e). The EXAFS curve of Ni_1/CdS NRs in Figure 3f clearly revealed that there was a Ni-O bond instead of a Ni-Ni or Ni-S bond in Ni_1/CdS, strongly demonstrating the atomic dispersion of Ni on CdS NRs by bonding with O. The synthesis mechanism of Ni_1/CdS by photochemical method was shown in Figure 2g. The atomically dispersed Ni ions were bonded with the surface hydroxyl groups generated during photochemical synthesis and the loading amount of Ni was up to 2.85%.

Under visible light (λ > 420 nm) irradiation, the Ni_1/CdS catalyst exhibited outstanding photocatalytic HER activity of 142.7 mmol g^{-1} h^{-1} and long-term stability up to 16 h.

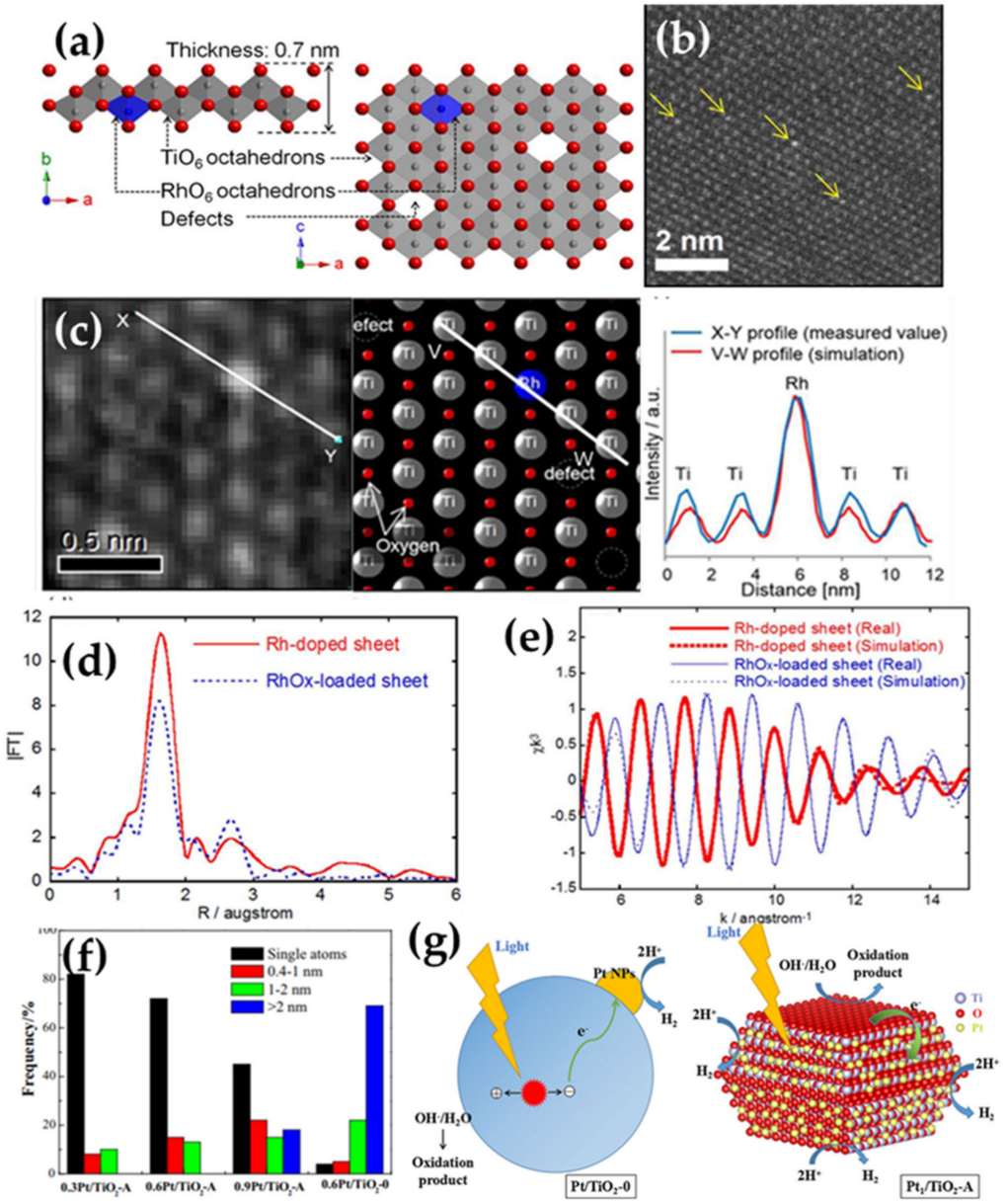

Figure 1. (**a**) Structural models of Rh-doped titania nanosheet from sectional view and plan view [36]; (**b**) HAADF-STEM (200 kV) image of Rh (x = 0.026)-doped $Ti_{1.82-x}Rh_xO_4$ nanosheet [36]; (**c**) magnified HAADF-STEM image (80 kV) and corresponding structural model of Rh (x = 0.026)-doped nanosheet, with intensity profiles along the line X−Y in the actually observed image and the line V−W in the simulated image [36]; (**d**) Fourier transforms of Rh K-edge k^3-weighted EXAFS for Rh (x = 0.026)-doped and RhO_x-loaded titania nanosheet [36]; (**e**) Inversely Fourier-transformed spectra for Rh-doped nanosheet and RhO_x-loaded nanosheet for the peak at around 2.8 Å in panel a [36]; (**f**) Size distribution of $0.3Pt_1/TiO_2$-A, $0.6Pt_1/TiO_2$-A, $0.9Pt_1/TiO_2$-A, and $0.6Pt/TiO_2$-0 [22]; and (**g**) Illustration of the charge transfer and H_2 evolution in Pt/TiO_2-0 and synthesized Pt_1/TiO_2-A [22].

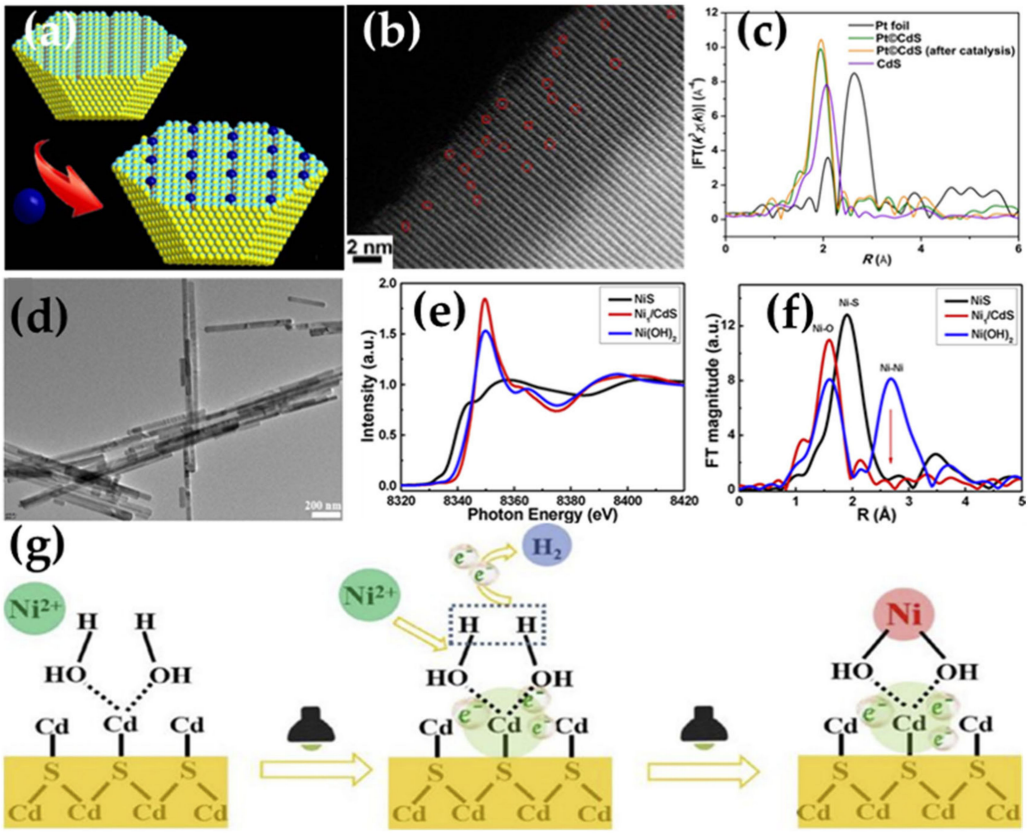

Figure 2. (**a**) The geometric models of isolated platinum atoms decorated on CdS surface with terraces [42]; (**b**) HAADF-STEM image in a spherical-aberration-corrected TEM for Pt©CdS [42]; (**c**) Fourier transform magnitudes of the experimental Pt L_3-edge EXAFS spectra of samples [42]; (**d**) TEM image of Ni_1/CdS composite [43]; (**e**) XANES spectra of NiS, Ni_1/CdS NRs and $Ni(OH)_2$ reference at Ni K-edge [43]; (**f**) The corresponding Fourier transform curves of EXAFS data [43]; (**g**) Schematic illustration of the preparation of Ni_1/CdS by photochemical method [43].

Apart from the studies mentioned above, other inorganic semiconductors, such as Bi_3O_4Br, $SrTiO_3$ and Cs2SnI6, have also been investigated as the support materials for constructing SAPCs [44,45]. Liu et al. successfully prepared a single-atom Co catalyst in which isolated Co atoms were incorporated into Bi_3O_4Br atomic layers (referred as Co-Bi_3O_4Br atomic layers) [46]. The Co atoms substituting Bi atoms were bonded with O atoms in a Bi_3O_4Br lattice. The isolated Co ions enriched the negative charges for Co-Bi_3O_4Br atomic layers and therefore boosted CO_2 adsorption and activation. Beneficial from the synergistic effect of the ultrathin structure and single-atom Co, Co-Bi_3O_4Br atomic layers exhibited enhanced photocatalytic CO_2 reduction activity compared to Bi_3O_4Br atomic layers and bulk Bi_3O_4Br.

2.1.2. Organic Materials

In recent years, organic polymer semiconductors, especially g-C_3N_4, have attracted extensive attention in photocatalysis owing to their fascinating advantages such as appropriate energy band structure, good stability, nontoxicity, low cost, etc. [47–49]. It is worth noting that the bandgap of pristine g-C_3N_4 is about 2.7 eV, with the lowest unoccupied molecular orbital (LUMO) and highest occupied molecular orbital (HOMO) well fitted for driving water splitting from the aspect of thermodynamics [50]. At the same time, g-C_3N_4 possesses abundant N atoms with lone-pair electrons, which are ideal coordinating sites for anchoring single metal atoms [51]. It has been found that the isolated metal atoms anchored on g-C_3N_4 can serve as active centers for boosting photocatalytic HER and ameliorate the low separation efficiency of photogenerated charge carriers for pristine g-C_3N_4 [52,53].

Hence, g-C_3N_4 has been intensively explored as the support materials for hosting single atoms, giving birth to various SAPCs.

Xiong et al. successfully incorporated Pt^{2+} into the pores of g-C_3N_4 by introducing Pt precursor prior to the polymerization of g-C_3N_4 (Figure 3a–c) [54]. The complete coordination of Pt^{2+} with N sites was formed before the formation of g-C_3N_4. They demonstrated that the metal-to-ligand charge transfer between Pt^{2+} and g-C_3N_4 facilitated photocatalytic HER. Further modification of g-C_3N_4 support with other coordinating atoms such as O and P can provide stronger anchoring ability for single atoms and improve the photocatalytic performance [55,56]. Au ions can be anchored on g-C_3N_4 by Au-N bond (referred as CNUAu) [57]. However, in the photocatalytic process, photogenerated electrons are inclined to transfer to Au(I) via Au-N bonds and reduce Au(I) to Au(0) atoms. The interaction between Au(0) and N atoms was too weak to prevent the agglomerate of free Au(0) atoms (Figure 3e). To deal with this problem, Xue et al. introduced active C-OH groups to g-C_3N_4 by pretreatment with H_2O_2 (referred as CNUH) prior to the impregnation synthesis of single-atom Au [55]. This enabled the immobilization of single Au(I) in g-C_3N_4 matrix through strong Au(0)-O bonds (referred as CNUHAu, Figure 3d). The stable and isolated Au(0) can act as efficient active sites for photocatalytic HER, allowing the oxygen-stabilized single-atom Au/g-C_3N_4 to exhibit excellent activities and stabilities.

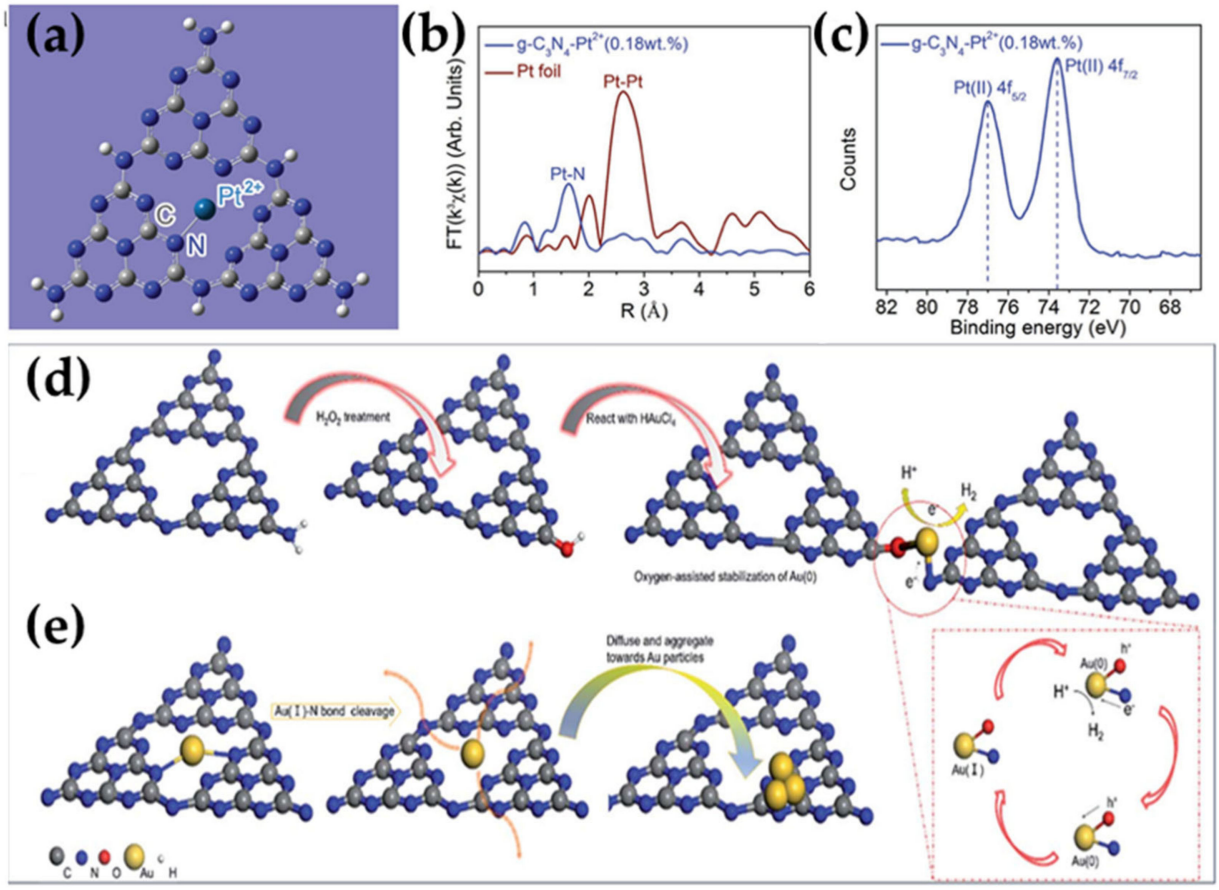

Figure 3. (**a**) Structural illustration for the coordination of g-C_3N_4 with Pt^{2+} [54]; (**b**) k^3-weighted Fourier-transform Pt L_3-edge EXAFS spectra for g-C_3N_4-Pt^{2+} (0.18 wt%) in reference to Pt foil (no phase corrected) [54]; (**c**) XPS Pt 4f spectrum of g-C_3N_4-Pt^{2+}(0.18 wt%) [54]; (**d**) Schematic of the structural evolution of CNUHAu during photocatalytic reactions [55]; (**e**) schematic of the structural evolution of CNUAu during photocatalytic reactions [55].

MOFs are one class of porous crystalline materials in which the metal ions/clusters and organic bridging molecules are combined by coordination bonds [58,59]. The porous structure of MOFs brings a large surface area, which is beneficial for adsorption of reactants [60,61]. Additionally, the skeleton structure and component of MOFs can be flexibly designed and modified. Introducing photosensitizers or other functional materials with single-site catalysts into MOF matrix is an efficient strategy for constructing SAPCs [62–64]. Ye et al. synthesized the porphyrin-based MOFs by integrating porphyrin-based molecular units (one kind of photosensitizers) and Zr_6 clusters into a three-dimensional network [65]. The resulting material exhibited excellent performance in visible-light absorption and CO_2 capture. On this basis, coordinatively unsaturated single-atom Co sites were further implanted into the porphyrin units (Figure 4a,b) to yield the single-atom Co/MOF photocatalyst (referred as MOF-525-Co), which exhibited significantly enhanced activity in photocatalytic CO_2 conversion. An advantage associated with the MOF support is that the individual photocatalytic active atoms can be stably anchored in the MOF matrix via applicable coordination bonds; this can lead to robust coordination and achieve ultrahigh loading of single atoms. For example, Zhou et al. firstly synthesized Pt single atoms coordinated on ultrathin 2D MOF nanosheets (denoted as PtSA-MNSs) (Figure 4c,d) [66]. The Pt atoms were anchored within the porphyrin rings before the formation of MOF, thus resulting in well-dispersed Pt single atoms with an ultrahigh loading of 12.0 wt% in the MOF nanosheets. Benefiting from the sufficient Pt single-atom active sites, the PtSA-MNSs exhibited record-high photocatalytic HER activity of 11320 umol g^{-1} h^{-1} under visible light irradiation.

Besides incorporating the single atoms to the MOF matrix, COFs composed of periodic organic building blocks showing abundant binding groups as well as a porous structure are also ideal for confining single atoms, by forming coordination between the isolated metal atoms and the heteroatoms in COFs framework [67,68]. Zhou et al. reported a photocatalyst constituted by a 2,2′-bipyridine-based COF bearing single Ni sites (Ni-TpBpy) (Figure 4e,f) [69]. The electrons can be transferred from photosensitizer to Ni sites and reduce CO_2 to CO under visible-light irradiation. The excellent activity (4057 umol g^{-1}, 5 h) was attributed to the synergistic effects of TpBpy favoring the adsorption and activation of CO_2 molecules (thus inhibiting the competitive H_2 evolution), and the single Ni catalytic sites that can facilitate the selective conversion of CO_2 (96%).

2.1.3. Carbon-Based Materials

Graphene-based materials such as GO and NG with excellent conductivity can be used as electron-transporting layers to accelerate the separation of photogenerated electron-hole pairs [70–72]. Through structural modification, the O atoms in GO and N atoms in NG can provide sufficient coordination sites for anchoring single atoms [73]. These support materials are often used as a bridge to promote the transfer of photogenerated electrons from photosensitizer to single-atom reaction sites [74]. For example, Xiong et al. immobilized isolated single Co atoms on GO nanosheets (referred as Co_1–G, Figure 5a–d) [75]. With the assistance of $[Ru(bpy)_3]Cl_2$ light absorber, the single Co sites in Co_1-G achieved unprecedented turnover frequencies of 3.77 min^{-1} in photocatalytic CO_2 conversion reactions. The authors further demonstrated that the C/O functional groups in GO served as robust ligands to anchor Co atoms, and the high conductivity of GO strongly facilitated the transfer of photoexcited electrons from $[Ru(bpy)_3]Cl_2$ to catalytic Co sites (Figure 5e). Xu et al. anchored single-atom Co on NG as a highly effective and durable cocatalyst for photocatalytic HER [76]. The Co-NG/CdS composite powder was further prepared by loading Co-NG on CdS. At a loading amount of 0.25 wt % for Co-NG, the hydrogen production rate of Co-NG/CdS was 3.42 and 1.3 times enhanced compared to NG-loaded CdS and Pt nanoparticle (1.5 wt %)-loaded CdS, respectively.

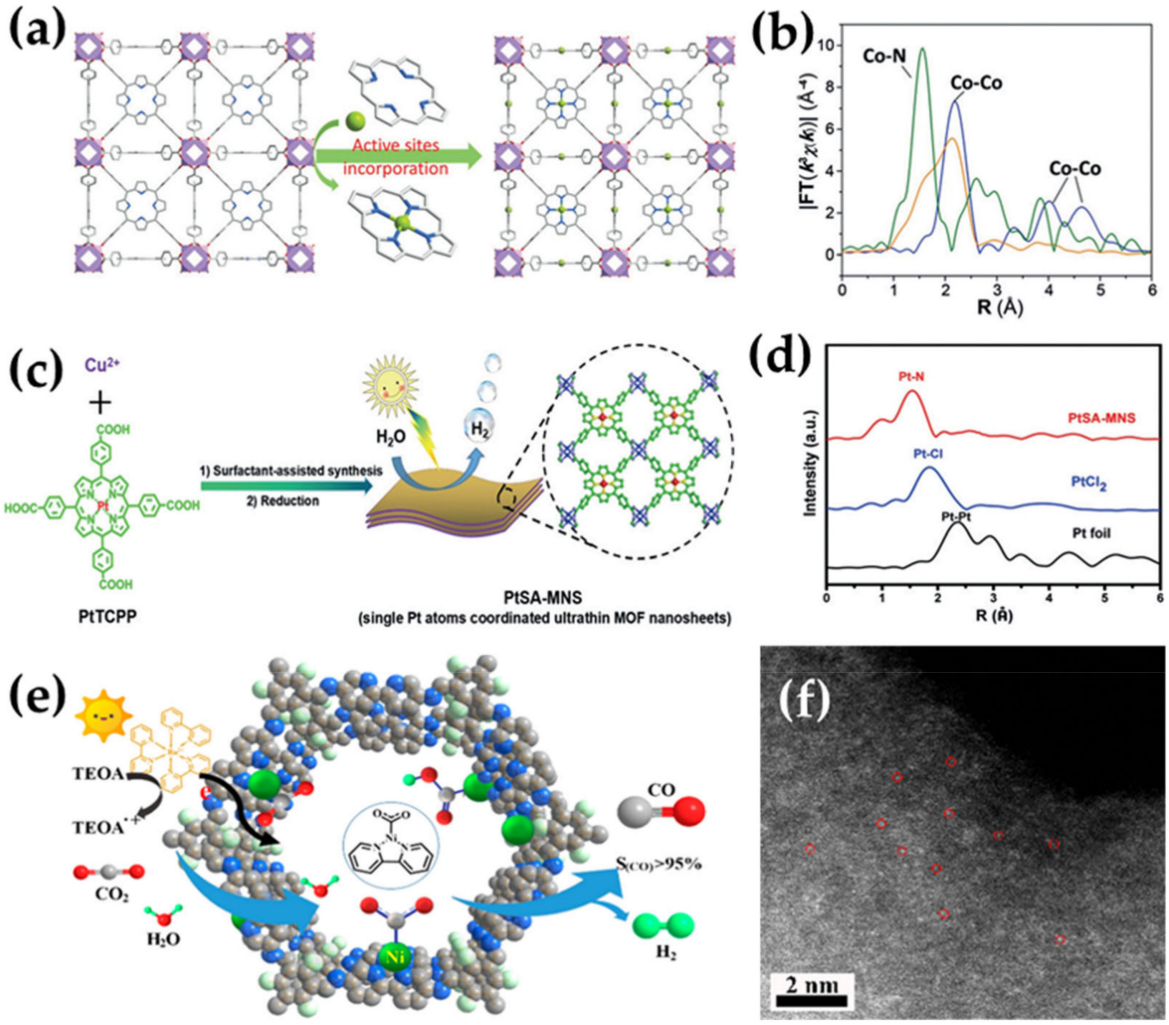

Figure 4. (**a**) View of the 3D network of MOF-525-Co featuring a highly porous framework and incorporated active sites [65]; (**b**) Fourier transform magnitudes of the experimental Co K-edge EXAFS spectra of samples (not corrected for phase shift). Key: Co foil (blue), Co@C (orange), MOF-525-Co (green) [65]; (**c**) Illustration of the synthetic route towards Pt single-atom coordinated ultrathin MOF nanosheets (PtSA-MNSs) through a surfactant-stabilized coordination strategy for photocatalytic hydrogen production [66]; (**d**) Pt L_3-edge EXAFS spectra for PtSA-MNSs, $PtCl_2$, and Pt foil [66]; (**e**) Schematic diagram of photocatalytic selective reduction of CO_2 over Ni-TpBpy [69]; (**f**) aberration-corrected HAADF-STEM image of Ni-TpBpy [69].

Carbon dots (CDs) are another attractive support material for hosting single atoms. Their bandgaps can be tuned by nitrogen doping to function as a good light-harvesting antenna [77]. Run Li et al. synthesized the CDs anchored with single Co atoms [78], in which the single Co atoms with a high loading content of 3.27% were stabilized through the $Co-N_4$ coordination structure. The authors unraveled that CDs played double functions in photocatalysis: the support for single-atom Co and the light-harvesting antenna. Meanwhile, the isolated Co atoms can boost the separation and directed migration of photogenerated charge carriers, and, more significantly, can gather the photogenerated holes for promoting oxidation reactions. As a result, the obtained photocatalyst exhibited excellent activity and stability in photocatalytic water oxidation (245 umol/g, 4 h), photocatalytic oxidative coupling of aromatic amines, and photodegradation of organic dye.

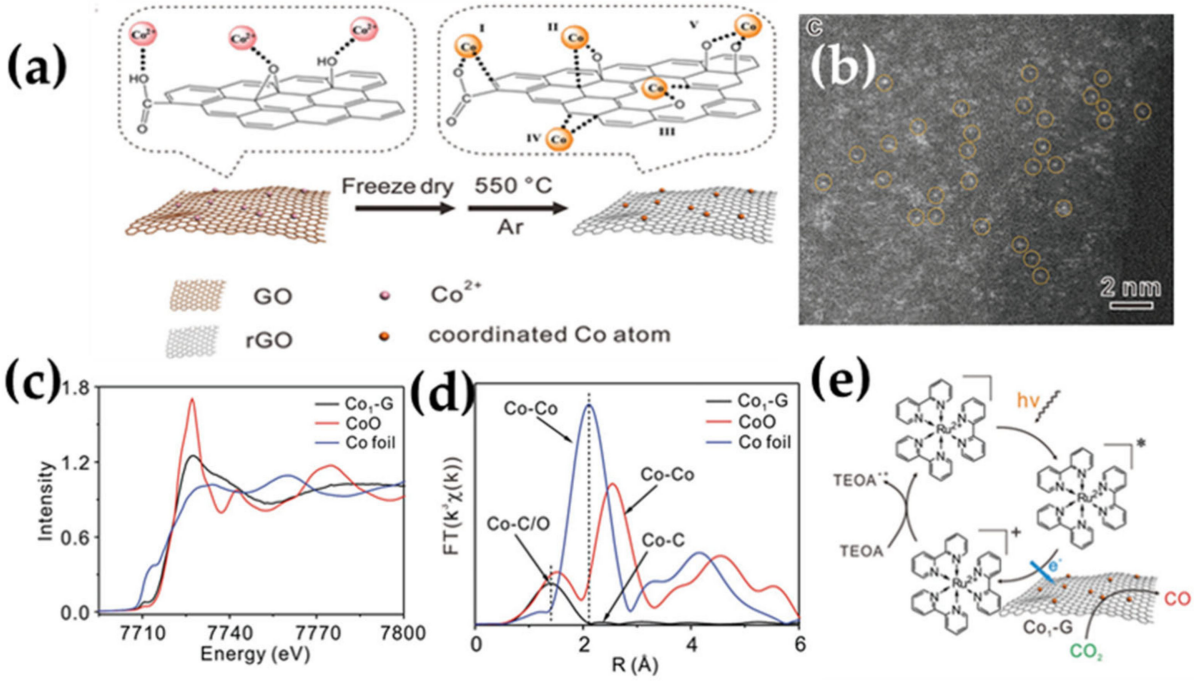

Figure 5. (**a**) Schematic illustration of the synthetic procedure for the Co_1–G catalyst [75]; (**b**) HAADF-STEM image of the Co_1–G catalyst. The atomically dispersed Co atoms are highlighted by the yellow circles [75]. (**c**) Normalized Co K-edge XANES spectra of the Co_1–G sample in reference to Co foil and CoO [75]; (**d**) k^3-weighted Fourier-transform Co K-edge EXAFS spectra [75]; (**e**) Schematic illustration of the process for photocatalytic reduction of CO_2 to CO using $[Ru(bpy)_3]Cl_2$ as a light absorber and Co_1–G nanosheets as a catalyst [75].

2.1.4. Metals

Aside from semiconductor materials, plasmonic metals such as Cu and Au nanocrystals can also be used as support materials for SAPCs. The single atoms are anchored within the metal support via metallic bond [79,80]. The strong interaction between light and plasmonic metals via LSPR effect can efficiently absorb light and generate a lot of hot electrons [81]. At the same time, the excellent electrical conductivity of metal and the metallic bonds can rapidly transfer the generated hot electrons to single-atom active sites for promoting photocatalytic reaction. Halas and colleagues prepared atomically dispersed Ru reactive sites on Cu antenna nanoparticles (Ru content below 0.2%, Figure 6a) for photocatalytic dry methane reforming [82]. The results of CO probe molecule diffuse reflectance infrared Fourier transform spectroscopy (CO-DRIFTS) coupled with density functional theory (DFT) calculations with van der Waals 'D3′ correction (Figure 6b) unambiguously uncovered the surface structure of Cu-Ru catalyst with atomically dispersed Ru. As shown in Figure 6c,d, compared to pure Cu and the Cu-Ru catalyst with high Ru loading ($Cu_{19.5}Ru_{0.5}$), the sparsely distributed single-atom Ru made the Cu-Ru catalyst present exceptionally high selectivity (>99%) and long-term stability (50 h) with greatly suppressed coking.

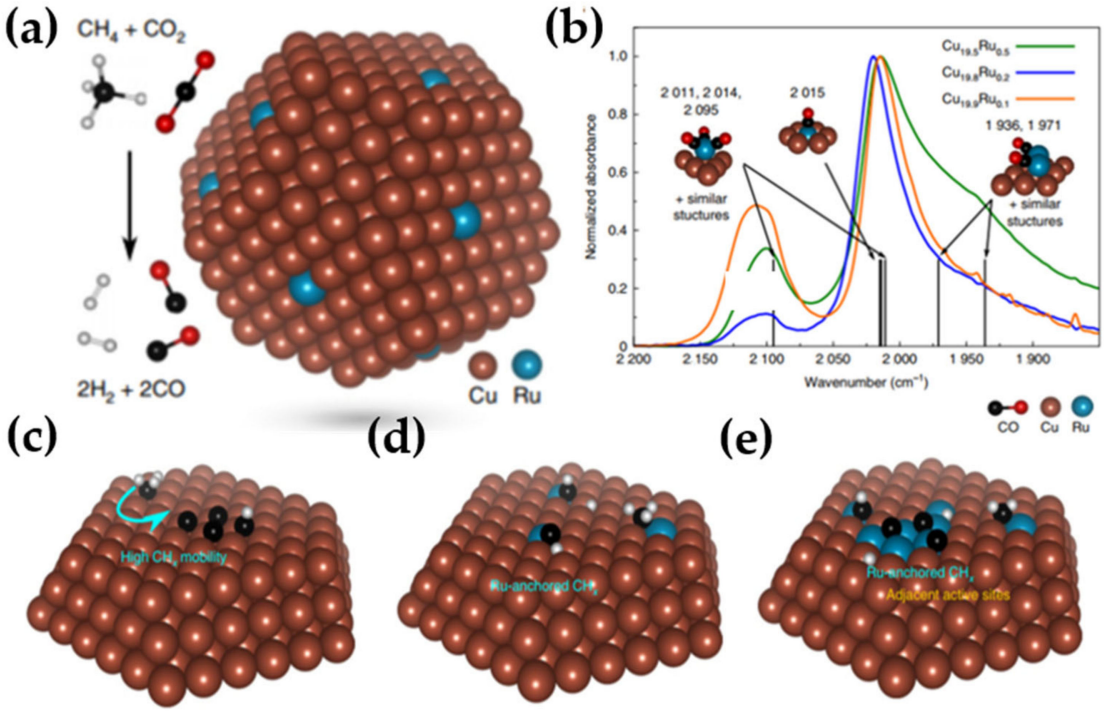

Figure 6. (**a**) Schematic of a Cu–single-atom Ru surface alloy catalyst with the dry reforming reactants and products shown on the left; (**b**) Infrared spectra of CO adsorbed on Cu–Ru catalyst surface at room temperature, and saturation coverage after a pretreatment at 200 °C in 10% CO in Ar (100 ml min^{-1}) for 1 h. Vertical lines located at the theoretical vibrational frequency of each structure are also shown. The relatively stronger peak at ~2100 cm^{-1} of $Cu_{19.9}Ru_{0.1}$ probably results from variations in Ru distributions during catalyst treatment; (**c**–**e**) Schematics of the compositional dependence of the Cu_xRu_y photocatalyst with respect to coke resistance: pure Cu (**c**), low Ru loading (**d**) and high Ru loading (**e**) [82].

2.1.5. Composites

In addition to single-component support, composite support, combining the advantages of multiple materials, is also promising for constructing SAPCs. An et al. anchored Pt single atoms on composites constituted by CDs and ultrathin CdS nanosheets (referred as CdS@CDs/Pt-SAs, Figure 7) [83]. The formation of Pt-S bonds between single Pt atoms and unsaturated S atoms of CdS accounted for the high stability of the catalysts. The presence of single Pt atoms promoted the directional migration of photogenerated electrons to Pt reaction sites for boosting HER. The addition of CDs slightly decreased the bandgap of CdS and was also favorable for charge separation. More importantly, it was found CDs were the key to facilitating the isolated dispersion of Pt on the surface of CdS. Experimental results showed that with the absence of CDs, Pt nanoparticles would be formed on the surface of CdS at a Pt loading amount of 1.15%. The CdS@CDs/Pt-SAs afforded an outstanding H_2 production rate (45.5 mmol g^{-1} h^{-1}) in photocatalytic reaction, 133 times higher than that of Cd@CDs.

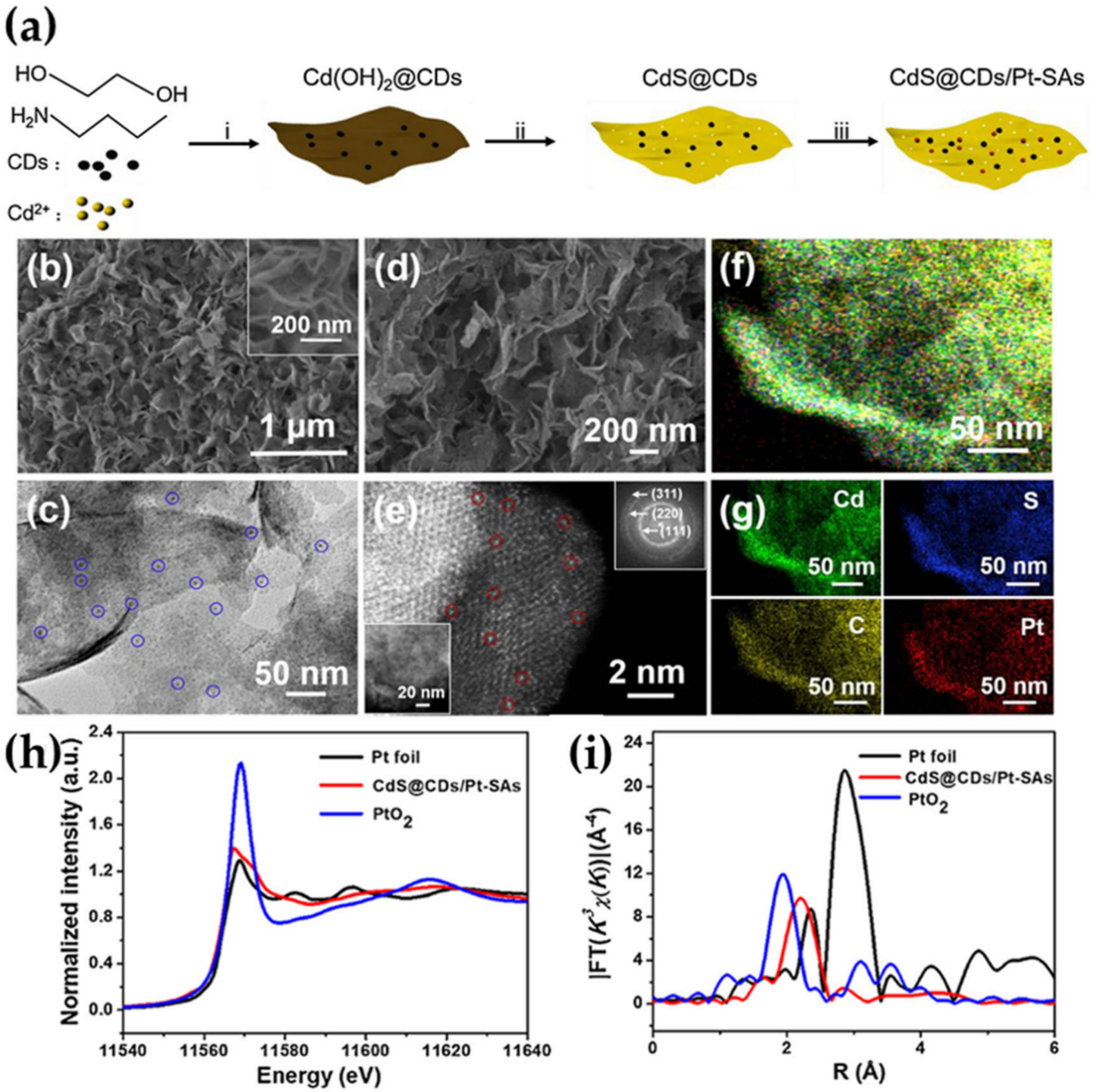

Figure 7. (**a**) Schematic illustration for the synthesis of CdS@CDs/Pt-SAs: (i) $Cd(OH)_2$@CDs was synthesized by the reaction of cadmium acetate with n-butylamine in a mixture of ethylene glycol and CDs aqueous solution via solvothermal method, (ii) Reaction of sulfidation process to produce CdS@CDs, (iii) Pt single-atoms were loaded by in-situ impregnation and conversion; (**b**) SEM image and (**c**) HRTEM image for $Cd(OH)_2$@CDs; (**d**) SEM image and (**e**) HAADF-STEM image of CdS@CDs/Pt-SAs. The insets show the HRTEM image (bottom-left), SAED pattern (up-right), and (**f**,**g**) EDS elemental mapping of CdS@CDs/Pt-SAs; (**h**) The normalized Pt-edge XANES spectra of different samples and reference; (**i**) Fourier transform magnitudes of the experimental Pt L3-edge EXAFS spectra of Pt foil, PtO_2, and CdS@CDs/Pt-SAs [83].

2.2. Single-Atom Cocatalysts

It is widely recognized that the presence of cocatalysts can effectively promote the kinetic process of photocatalysis and is significantly important for achieving high overall photocatalytic efficiency [84]. In general, loading of metal cocatalysts can bring about the following two functions: (1) the metal cocatalysts can serve as electron traps and induce the directional migration of photogenerated electrons from semiconductor to metal, thus suppressing the recombination of photogenerated electrons and holes and prolonging the lifetime of these charge carriers; and (2) the cocatalyst can reduce the adsorption and activation energies toward reactants and serve as the reaction centers for surface photocatalytic reaction [85,86]. Considering that only the surface atoms of cocatalyst particles participate in the catalytic reaction, the atomic dispersion of cocatalyst in SAPCs can realize maximized atomic utilization and lower the cost of the noble catalyst [87]. In addition to these advantages, single-atom cocatalysts will exhibit unexpected photocatalytic activity and selectivity due to the unsaturated coordination condition and tunable electronic structures derived from the interaction with supports [88]. The strong interaction between the single metal atoms and the support in SAPCs are also effective means to modulate the charge kinetics, which is critical for the overall conversion efficiency of photocatalysis [89,90]. In addition, the interaction between single metal atoms and supports can also contribute to adjusting the energy band structure and expanding the spectrum of light absorption of supports [91,92]. Hence, SAPCs as a new paradigm of cocatalyst/photocatalsyt composite promise to exhibit excellent photocatalytic activity, selectivity, and durability [93]. In the following, the various single metal atoms applied as cocatalysts in SAPCs are discussed in terms of noble metals and non-noble metals.

2.2.1. Noble Metals

Due to their suitable Fermi level for trapping electrons and a low potential for H_2 evolution, noble metal Pt is an efficient cocatalyst for H_2 evolution and has been intensively studied in SAPCs [94–97]. Wu et al. reported a photocatalyst with significantly enhanced photocatalytic activity and maximized utilization of Pt [98], in which the isolated Pt atoms were incorporate into the sub-nanoporosity of 2D g-C_3N_4 (referred as Pt-C_3N_4, Figure 8b) and acted as co-catalyst for photocatalytic HER. The intrinsic change of the surface trap states induced by single-atom Pt contributed to a longer lifetime of photogenerated electrons, which was the primary factor for the prominently improved photocatalytic performance. Bi et al. further investigated the in situ charge transfer and chemical bond evolution between the single-atom Pt and g-C_3N_4 during photocatalytic HER (Figure 8a) [99]. The results showed that different from the metallic Pt decorated-g-C_3N_4 catalyst, within single-atom Pt/C_3N_4, the Pt-N bond broke to form Pt^0 species and the C-N bond transformed into C=N bond of g-C_3N_4 under visible light irradiation. Such dynamic changes designated Pt^0 and g-C_3N_4 as the reaction sites for reduction and oxidation reactions respectively, and this contributed to the remarkably enhanced H_2 evolution activity. Furthermore, it has been demonstrated that a higher loaded content of Pt single atoms can give much higher photocatalytic activity. For example, Zhou et al. developed a surfactant-stabilized coordination strategy to realize ultrahigh single-atom Pt loading of 12% within MOFs [66]. The resulting SAPCs exhibited an exceptionally high activity of 11320 umol g^{-1} h^{-1} for photocatalytic HER under visible light.

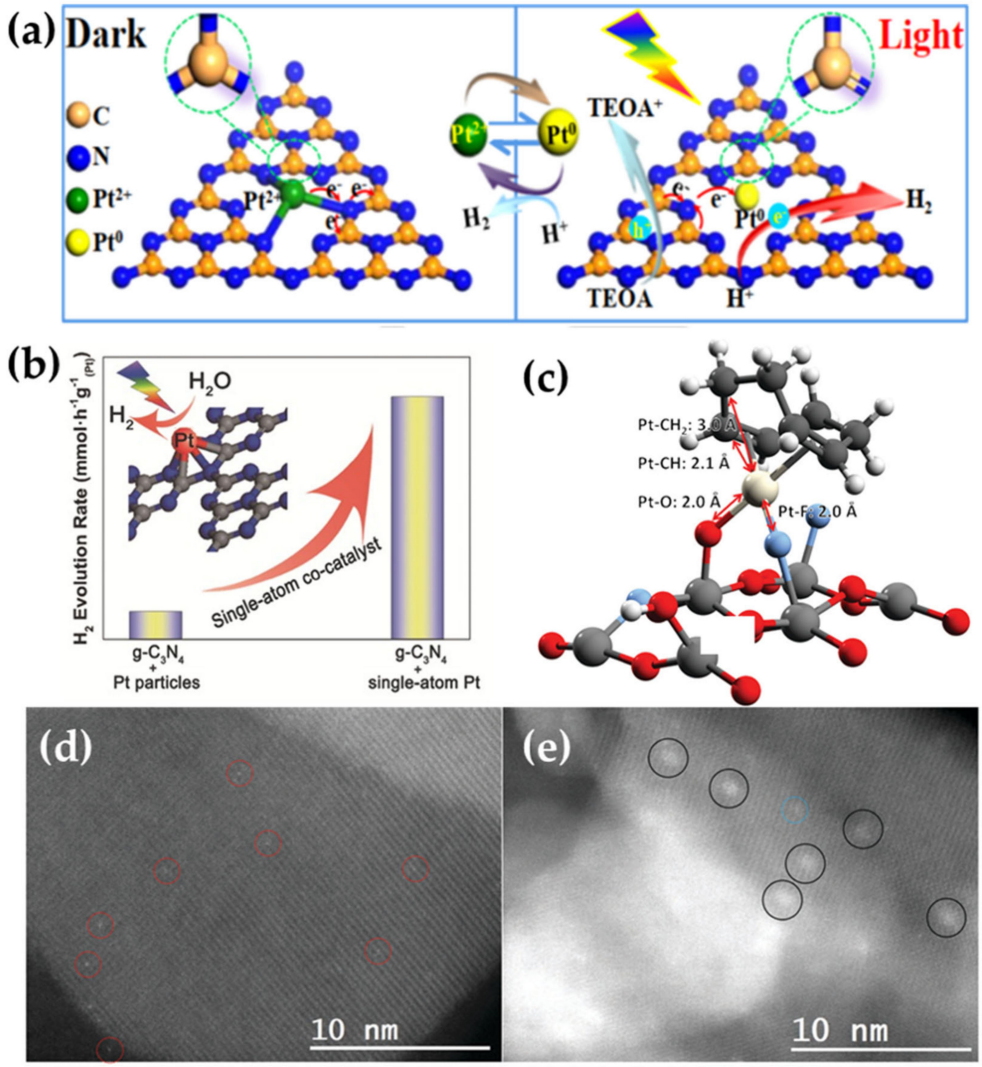

Figure 8. (**a**) Illustration of the charge transfer and bond variation on S-Pt-C_3N_4 catalysts for photocatalytic hydrogen evolution [99]; (**b**) Photocatalytic activity comparison of g-C_3N_4 with Pt nanoparticles and single atoms, respectively. Inside is the structure model of Pt-C_3N_4 [98]; (**c**) O–Pt–F DFT-optimized structure, used as the initial model for EXAFS fitting; (**d**,**e**) HAADF-HRSTEM images of the 0.5%Pt_{GR}:TiO_2 [100]; (**d**) and 0.5%Pt_{NP}:TiO_2 (**e**). Single atoms are denoted by red circles, clusters by blue circles, and nanoparticles by black circles [100].

Apart from the bonding of single-atom Pt with the coordinating atoms within supports, isolated Pt complex can also be anchored on the support and act as reaction sites. Jean-Marie Basset et al. prepared Pt single atoms for photocatalytic water splitting via the surface organometallic chemistry (SOMC) technique [100]. The Pt complex (1,5-cyclooctadiene)dimethylplatinum(II) ($(CH_3)_2Pt(COD)$) was grafted on anatase TiO_2 with highly exposed (001) facets (referred as Pt_{GR}:TiO_2) (Figure 8c,d). Compared to the photocatalyst synthesized by impregnation method with the same Pt loading amount (referred as 0.5%Pt_{NP}:TiO_2, Figure 8e), Pt in 0.5%Pt_{GR}:TiO_2 was atomically distributed, leading to excellent activity for photocatalytic HER and effectively suppressing side reaction between H_2 and O_2 forming H_2O in dark conditions. However, the problem is that in this system the anchoring effect for the single SOMC-grafted Pt atoms was weak, and as a result the Pt atoms rapidly aggregated and formed nanoparticles under photocatalytic conditions.

In addition, Pd, Ru, Rh, and Au have also been applied in the study of SAPCs for photocatalytic water splitting [101–103]. Single-atom Pd catalysts have shown good potential for photocatalytic reduction reactions. In the study carried out by Chen [104], single Pd atoms were intercalated into the space among the adjacent layers of g-C_3N_4 and anchored

on the surface of g-C_3N_4 simultaneously through a photo-deposition method (referred as Pd-g-C_3N_4, Figure 9a). This distinct structure facilitated the charge transfer from the bulk interior to the outermost surface where single Pd atoms acted as reactive sites for sequential reactions. The Pd/g-C_3N_4 photocatalyst exhibited more efficient photocatalytic hydrogen evolution than that of the optimal Pt loaded Pt/g-C_3N_4 benchmark (synthesized by the same photo-deposition method). Yan et al. developed a photocatalyst with high-valence single-atom Ru(IV) intercalated in a two-dimensional GaS nanosheet for photocatalytic HER (Figure 9b,c) [42]. The intercalated single-atom Ru possessed a hexagonal structural configuration of Ru_1-S_6, which served as a fast electron channel for rapid segregation and transfer of photogenerated carriers in photocatalytic process. As a result, the photocatalytic activity of H_2 production under visible light was 30 times higher than that of the pure GaS nanosheet. Ishihara et al. introduced isolated single-atom Rh dopants in TiO_2 nanosheet [27], and this led to 10 times higher photocatalytic activity for H_2 evolution than that of undoped TiO_2 nanosheet. More interestingly, developing bifunctional single-atom redox sites in one photocatalyst would significantly enhance the dynamics of photocatalytic water splitting [105,106]. Liu et al. introduced Pt and Au dual single atoms within g-C_3N_4 in order to construct bifunctional redox sites [107]. The resulting catalysts, referred to as Pt-Au/g-C_3N_4, realized spontaneous overall water splitting, opening a new prospect for the application of SAPCs (Figure 9d).

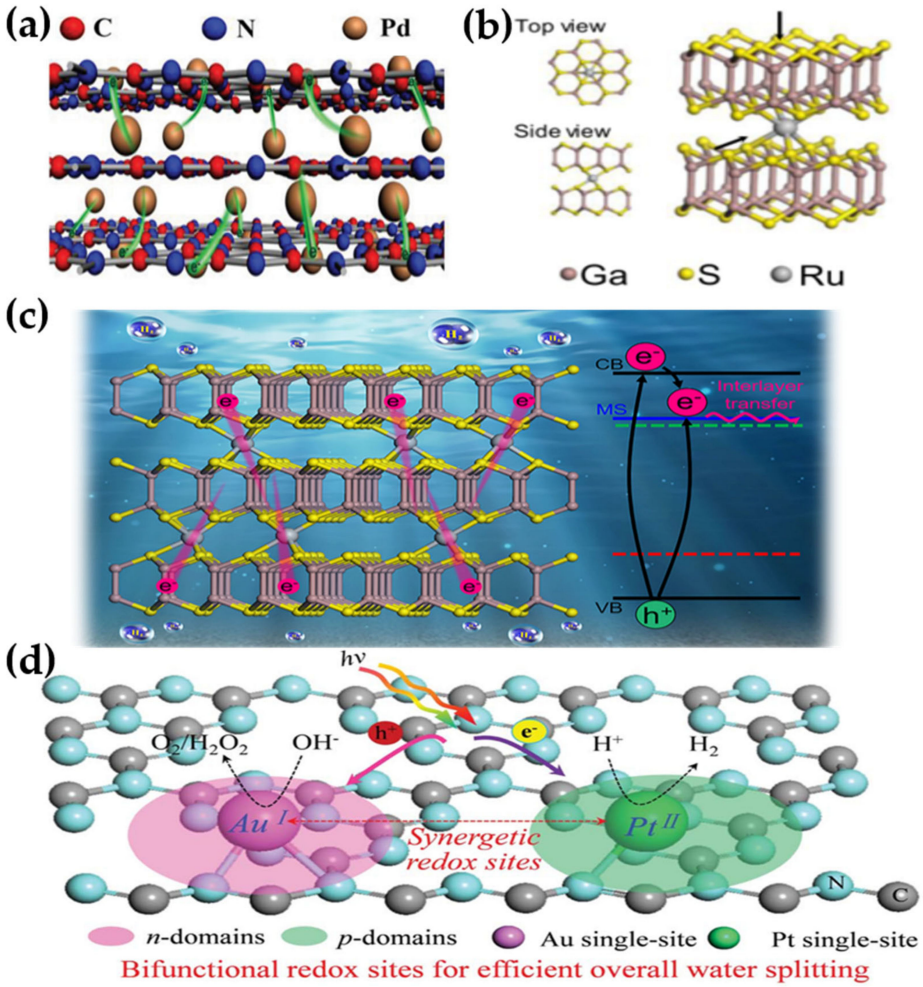

Figure 9. (**a**) Conceptual illustration of Pd/g-C_3N_4 hybrid with the interlayer intercalation and surface anchor of Pd atoms [104]; (**b**) Structural model of the Ru−GaS NSs [40]; (**c**) Schematic diagram of photocatalytic HER over single-atom Ru(IV) intercalated GaS nanosheet [40]; and (**d**) Schematic of the solar-driven overall water splitting for synergetic bifunctional Pt–Au redox single sites [107].

2.2.2. Non-Noble Metals

Non-noble metal cocatalysts with lower prices and more abundant reserves can dramatically reduce the cost of the widely studied photocatalysts that utilize precious metals as cocatalysts [108]. In particular, the non-noble transition metals with vacant orbitals can be used as electron traps to receive electrons [109,110]. In some cases, the non-noble metal cocatalyst exhibited even superior performance than that of noble metal cocatalysts.

Co is a frequently explored non-noble cocatalyst in photocatalysis. The single-atom Co photocatalysts with isolated Co sites cooperated with photoactive supports enabled photocatalytic water splitting and CO_2 fixation reactions. Wei et al. developed a Co_1-N_4 single-site photocatalyst via atomic layer deposition (ALD), in which the single-atom Co was anchored on phosphorus-doped g-C_3N_4 support (referred as Co_1/PCN, Figure 10a–c) [111]. The phosphidation treatment of g-C_3N_4 support improved the separation and transfer of photogenerated carriers. Atomically dispersed Co atoms were stably immobilized on g-C_3N_4 nanosheets by forming covalently bonded Co_1-N_4 structure. The coordinated donor N increased the electron density of Co and lowered the formation barrier of the key Co-H intermediate, consequently boosting H-H coupling and H_2 evolution in photocatalytic reaction. On this basis, the authors further developed another photocatalyst with single site Co_1-phosphide anchored on phosphorus-doped g-C_3N_4 support through Co-P_4 bonds (referred as Co_1-phosphide/PCN, Figure 10d) [56]. Compared to Co_1-N_4, the coordinatively-unsaturated Co_1-P_4 single sites were more favorable for water molecular adsorption and activation in oxygen evolution reaction. Therefore, Co_1-phosphide/PC_3N_4 afforded a more stable and higher photocatalytic activity. Huang et al. developed a single-site MOF photocatalyst, in which single-atom Co and Ru-based photosensitizers were incorporated into an MOF matrix (referred as Co-Ru-UIO-67(bpy)) [112]. They demonstrated the exceptional catalytic activities of Co-Ru-UIO-67(bpy) and established the fundamental structure−function relationships of this system for HER. Li et al. employed g-C_3N_4 to anchor the Co^{2+} sites and harvest visible light [113]. The photocatalyst was synthesized by a simple photo-deposition method and exhibited excellent activity (0.128 umol/mg) and high selectivity for CO in photocatalytic CO_2 reduction.

Other transition metals such as Cu, Ni, Fe, etc. have also been applied in SAPCs and exhibited excellent photocatalytic performance. For example, Hyeon et al. demonstrated that a reversible and cooperative photoactivation process occurred on anatase TiO_2 incorporated with single Cu atoms (referred as Cu/TiO_2) [114]. During the photocatalytic process, the photogenerated electron from TiO_2 was localized into the Cu $d_z{}^2$ state and changed the valence state of single-atom Cu in Cu/TiO_2. Because of the axial antibonding character of Cu $d_z{}^2$ state, valence state change of Cu would leaded to a lattice distortion in the adjacent TiO_2, which activated the adjacent TiO_2 and significantly enhanced photocatalytic performance. The localized electrons were consumed after reduction reactions and the single Cu atoms return to the Cu^{II}state. Similarly, through tuning the oxidation state of Ni, the photocatalytic performance of SAPCs can be efficiently improved [115]. Shi et al. constructed partially oxidized Ni single-atom sites on g-C_3N_4 (referred as g-C_3N_4-0.2Ni-HO) and achieved over 30 times enhancement for photocatalytic HER performance [116]. They revealed that the unpaired d-electrons in 3d orbital of partially oxidized Ni single atoms can be excited under irradiation, leading to enhanced light absorption, charge separation and transportation. Therefore, the photocatalytic HER performance of g-C_3N_4-0.2Ni-HO was significantly improved. Fu and colleagues fabricated a photocatalyst with single-atom Fe anchored on crimped g-C_3N_4 (referred as Fe@g-C_3N_4) for photocatalytic HER [117]. The appropriate d-band position and negatively shifted Fermi level of Fe@g-C_3N_4 effectively enhanced photocatalytic HER rate (3390 mol h^{-1} g^{-1}, $\lambda > 420$ nm), giving an apparent quantum efficiency (AQE) value of 6.89% at 420 nm.

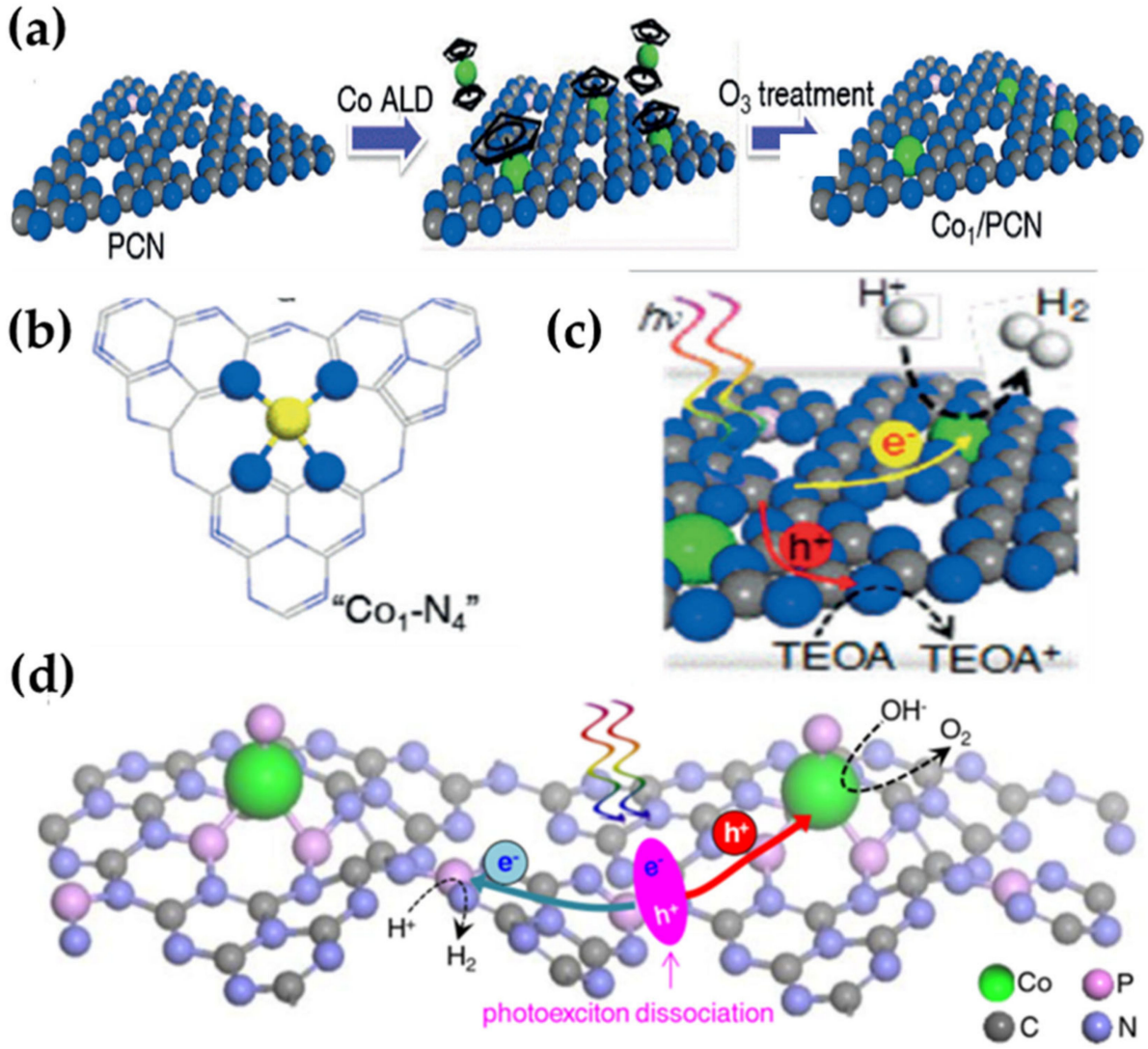

Figure 10. (**a**) Illustration of the synthesis for a single-site Co_1/PCN catalyst by the ALD method [111]; (**b**) Top view of the model structures: "Co_1-N_4" [111]; (**c**) Illustration of photocatalytic H_2 production of Co_1/PCN [111]; (**d**) Schematic illustration of the solar-driven overall water splitting on Co_1-phosphide/PC_3N_4 photocatalyst, where the photogenerated electrons and holes are spatially separated and transferred to active sites to drive HER and OER [56].

3. Synthesis of SAPCs

A simple and effective synthesis method is one critical factor for the practical application of SAPCs [118]. It is essential to construct strong coordination interactions between single metal atoms and support materials to avoid the aggregation of these isolated atoms with high surface free energy during synthesis and reaction processes [119]. This can be achieved through various strategies including defect engineering, coordinated design, and spatial confinement [120]. In the following section, the commonly used synthesis methods for SAPCs are summarized.

3.1. Impregnation Method

The impregnation method is a typical and flexible method for the synthesis of single-atom catalysts. The support materials are immersed in a solution containing appropriate metal precursors. In this condition, the metal ions could be anchored or absorbed on the support surface through coordination, electrostatic adsorption, or spatial confinement. This is followed by drying and activation treatment, which can make the single metal atoms stably anchored on the supports. Here, the bonding with coordination atoms in supports such as, O, N, P, S, etc. is the key to keep the metal atoms spatially isolated with restricted migration.

Supports with high specific surface areas and sufficient coordination sites, such as g-C_3N_4, GO, NG, MOF, TiO_2, etc., are suitable supports for SAPCs synthesized via the impregnation method. Wang et al. explored zirconium-porphyrinic MOF hollow nanotubes (HNTM) as the support materials [121]. Benefitting from the well-defined square-planar anchoring sites of porphyrin units, a series of noble-metal (Ir, Pt, Ru, Au, and Pd) single atoms were successfully immobilized on HNTM structures by the simple impregnation method (Figure 11a). In some cases, when the coordination between single metal atoms and supports cannot be established under room temperature, appropriate heat treating is required to promote the bond formation. Xu et al. prepared atomically dispersed Ni atoms on nitrogen-doped graphene (referred as Ni-NG) by the impregnation method [122]. In a typical synthesis, the GO support was dispersed in $NiCl_2$ aqueous solution by sonication treatment to make Ni^{2+} uniformly and atomically adsorbed on the support. Thereafter, the sample was collected and freeze-dried, followed by treatment in NH_3 atmosphere for doping N into GO and establishing a strong interaction between Ni and the N-doped GO support. The prepared Ni-NG sample was further coupled with CdS and employed as an active non-noble-metal cocatalyst for photocatalytic HER. The results showed that Ni-NG/CdS exhibited much improved stability and activity (1351.1 umol/h) compared to noble metal Pt loaded-CdS, and this can be attributed to the beneficial effects associated with the single Ni atoms anchored on NG.

3.2. Co-Precipitation Method

As for the co-precipitation method, single atoms are immobilized on the supports during their formation process. This method is suitable for support materials such as g-C_3N_4, MOF, metal sulfides, and metal [123–125]. For example, Lu et al. prepared a series of single-atom Mo catalysts by calcining low-cost primary material of urea with various amounts of Mo(VI) salts [126]. The isolated Mo atoms were incorporated into g-C_3N_4 through MoN_2 species in the polymerization process. The coordinatively unsaturated Mo sites acted as reaction centers for N_2 chemisorption and activation during photocatalysis. With regard to the metal supports, the atomic ratio of metal precursor to support is a key factor that should be precisely controlled for preparation of single atoms in metal supports. For example, Yang et al. synthesized a single-atom Pt_1Ag_{24} alloy cocatalyst on g-C_3N_4, and the resulting composite (referred as Pt_1Ag_{24}/ g-C_3N_4) was applied in photocatalytic HER [127]. The H_2 evolution rate of Pt_1Ag_{24}/g-C_3N_4 reached 39.7 umol/h, which was four times higer than that of Ag_{25}/g-C_3N_4. The precise composition of single-atom Pt_1Ag_{24} alloy cocatalyst was tuned by carefully tuning the molar ratio of Ag and Pt precursors during the nucleation and growth process.

3.3. Photo-Deposition Method

Similar to the impregnation method, the photo-deposition approach is also carried out in solution, but uses the energy of photons to reduce and anchor metal ions on the support. It is a mild and economical preparation method [128]. Moreover, this method is favorable for increasing the loading content of single metal atoms. Guo et al. anchored single-atom Pt on N-vacancy-riched g-C_3N_4 by a icing-assisted in-situ photocatalytic reduction method at sub-zero temperature [129]. The schematic illustration of photoreduction of H_2PtCl_6 on g-C_3N_4 is shown in Figure 11b. Under illumination, the $[PtCl_6]^{2-}$ adsorbed on g-C_3N_4 was reduced to metal Pt species by photogenerated electrons from excited g-C_3N_4. Because of the facile diffusion and nucleation of Pt species, the Pt nanoparticles was readily generated in solution. However, only the $[PtCl_6]^{2-}$ species absorbed at N vacancies could be reduced into single-atom Pt under icing conditions. Moreover, a strong reactive metal-support interaction was formed between Pt single atoms and g-C_3N_4 due to the rich N vacancies, and this contributed to an ultrahigh average covering density of PtSAs (0.35 mg m^{-2}) on the electron-deficient g-C_3N_4. In addition, it has also been demonstrated that the metal ions could be precisely deposited on the electronic enrichment area in photochemical reduction process, which is expected to enable the position-controlled deposition of single atoms [130,131].

3.4. Atomic Layer Deposition Method

Atomic layer deposition (ALD) is a precise technology in which the steam of a metal precursor is controlled deposited on the support in the reaction chamber. By altering the reaction temperature, deposition time, and deposition cycles, single-atom photocatalysts have been successfully synthesized via the ALD method [132,133]. For example, Sun et al. utilized ALD to produce isolated Pt single atoms and clusters on NG nanosheets. [134] The typical process for ALD is shown in Figure 11c. The Pt precursors ($MeCpPtMe_3$) were firstly reacted with NG nanosheets. Subsequently, they were completely oxidized in the presence of O_2 to result in the single Pt atoms. These two steps formed a complete cycle of ALD. By exactly adjusting the cycle number, the size and density of Pt on NG can be intentionally tuned from single atoms, sub-nanometre clusters, to NPs. However, it should be noted that ALD is relatively more complex and expensive compared to the other commonly used methods for constructing SAPCs [135].

3.5. Other Methods

In addition to the above widely explored methods, some distinct novel synthetic strategies have also been developed by researchers to create SAPCs. For instance, Zhang et al. fabricated SAPCs with an ultrahigh Pt loading content of 8.7 wt % via ion exchange between Pt^{2+} and the alkali metal ions K^+ that were intercalated into carbon nitrides (referred as SA-Pt/g-C_3N_4-8.7, Figure 11d) [136]. The spatial confinement within adjacent layers of support was important factor for achieving atomic dispersion of Pt with an ultrahigh loading content. Moreover, the well-confined interlayer environment alerted the charge distribution around the Pt atoms, and this favored proton adsorption as well as lowered the energy barrier of HER. Hence, SA-Pt/g-C_3N_4-8.7 exhibited an excellent activity of 22.5 mmol g^{-1} h^{-1} and an apparent quantum yield of 22.5% for photocatalytic HER, which are record-breaking for the reported g-C_3N_4-based photocatalysts.

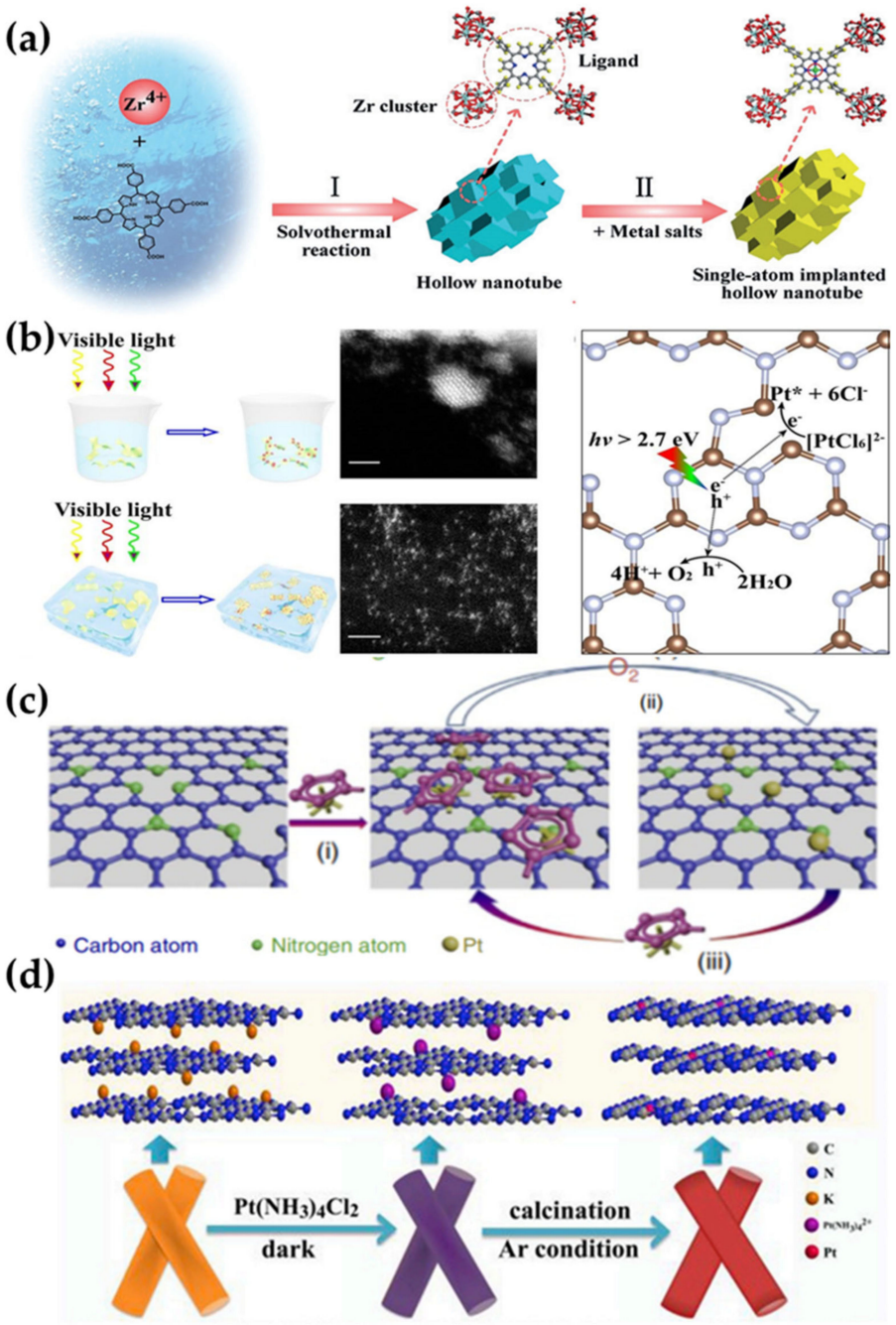

Figure 11. (**a**) Formation of the hollow nanotube MOF and the single atom-immobilized hollow nanotube MOF, which are denoted as HNTM and HNTM-M, respectively [121]; (**b**) Schematic illustration of the icing-assisted in-situ photocatalytic reduction method for preparing the supra-high-density PtSAs-loaded g-C_3N_4. Scale bar: 2 nm [129]; (**c**) Schematic illustration of the ALD mechanism for creating Pt single atoms on NGNs [134]; and (**d**) Illustration of the synthetic process of single-atom Pt photocatalysts [136].

4. Applications of SAPCs for Photocatalytic Water Splitting

H_2 produced from photocatalytic water splitting is an ideal clean energy to replace fossil fuels. However, great challenges remain for developing high-activity, durable, and economical photocatalysts that can realize practical applications toward photocatalytic H_2 generation. The creation of SAPCs provides a new clue for the development of water splitting photocatalysts with excellent activity, selectivity, and stability, as well as high atomic utilization of noble metals to lower the cost of the catalyst. Table 1 summarizes the recent progress in this research area. As discussed above, the single metal sites in SAPCs have been intensively used as efficient cocatalysts for promoting photocatalytic H_2 evolution.

In particular, benefitting from the high redox potential and work function, Pt in the form of atomically dispersed single atoms on TiO_2, g-C_3N_4, and MOF have manifested excellent performance in photocatalytic H_2 evolution [137,138]. Li et al. reported an efficient photocatalyst (referred as Pt_1/def-TiO_2) by dispersing single Pt atoms on defective TiO_2 [94]. Due to the hydrogen spillover effect, the atomically dispersed Pt atoms caused the formation of surface oxygen vacancies in neighboring TiO_2 units, giving birth to the Pt-O-Ti^{3+} atomic interface. According to the experimental results and DFT calculations, the Pt-O-Ti^{3+} atomic interface effectively facilitated the transfer of photogenerated electrons from Ti^{3+} defective sites to single Pt atoms, thereby enhancing the separation of electron-hole pairs. This unique structure allowed Pt_1/def-TiO_2 to exhibit an exceptionally high turnover frequency of 51,423 h^{-1}, which was 591 times higher than that of the Pt nanoparticles-supported TiO_2 photocatalyst.

SAPCs with non-noble metals such as Co, Ni, etc. have also been developed as cocatalysts to give excellent performance in photocatalytic water splitting. Importantly, apart from the benefits for H_2 evolution reaction, it has been reported that the cocatalyst of single-atom Co could facilitate the oxidation of water for O_2 evolution half reaction or even overall water splitting [139]. For example, Wei et al. developed a single-atom, Co-based photocatalyst (referred as Co/g-C_3N_4) with single Co atoms confined within phosphide doped-g-C_3N_4 nanosheets. [56] The Co_1-phosphide sites with coordination unsaturated Co sites exhibited oxygen evolution activity by effectively promoting water molecular adsorption and activation, and also helped to suppress electron-hole recombination. Meanwhile the phosphide dopants accelerated the electric conductivity of Co/g-C_3N_4. As a result, in photocatalytic overall water splitting reaction, Co/g-C_3N_4 afforded a H_2 evolution rate as high as 410.3 umol h^{-1}, with the carrier lifetime over 20 times prolonged compared to the pristine g-C_3N_4.

Table 1. Summary of SAPCs for photocatalytic water splitting. The order is arranged by the time of publication.

	Supports	Single Atoms	Coordination	Loaded Content	Synthesis Methods	Products	Production Rate	AQE
1 [27]	TiO_2 nanosheet	Rh	Rh-O	2.6 at.%	co-precipitation	H_2	51 umol h^{-1}	/
2 [98]	g-C_3N_4	Pt	Pt-N	0.16 wt.%	impregnation	H_2	318 umol h^{-1}	/
3 [54]	g-C_3N_4	Pt^{2+}	Pt-N	0.18 wt.%	co-precipitation	H_2	605 umol g^{-1} h^{-1}	/
4 [113]	g-C_3N_4	Co	Co_1-N_4	1 wt.%	ALD	H_2	10.8 umol h^{-1}	10.3%, 420 nm
5 [127]	Ag cluster	Pt	Pt-Ag	4 at.%	co-precipitation	H_2	39.7 umol h^{-1}	/
6 [56]	P doped g-C_3N_4	Co	Co_1-P_4	0.40.%	impregnation	H_2. O_2	126.8 umol g^{-1} h^{-1}	0.16%, AM 1.5 illumination
7 [96]	g-C_3N_4	Pt	Pt-N (maybe)	/	impregnation	H_2	12.7 umol g^{-1}, 4 h	/
8 [22]	TiO_2	Pt	Pt-O	0.6 wt.%	photo-deposition	H_2	85.4 umol h^{-1}	/
9 [76]	NG	Co	/	0.25 wt.% (Co-NG)	impregnation	H_2	1382 umol h^{-1}	50.5%, 420 nm
10 [104]	g-C_3N_4	Pd	surface:Pt-N;interlayer: Pt-N, Pt-C	0.33 wt.%	photo-deposition	H_2	6688 umol g^{-1} h^{-1}	4%, 420 nm
11 [137]	g-C_3N_4	Pt	Pt_1-N_4	0.11 wt.%	photo-deposition	H_2	42.1 umol h^{-1}	/
12 [95]	Al- porphyrinic MOF	Pt	Pt-N	0.29 wt.%	impregnation	H_2	129 umol g^{-1} h^{-1}	/
13 [121]	Zr–porphyrinic MOF	Ir, Pt, Ru, Au, Pd	Pt-N_4Cl_2	1.41 (Ir), 2.74 (Pt), 1.92 (Ru), 1.18 (Au), 3.68 (Pd), wt.%	impregnation	H_2	201.9 umol g^{-1} h^{-1}	/
14 [138]	g-C_3N_4	Pt^{II}	Pt-N	/	impregnation	H_2	140 umol g^{-1} h^{-1}	1.5%, 420 nm
15 [35]	mesoporous TiO_2	Cu	Cu-$O_{2.5}$	<0.3 wt.%	impregnation	H_2	/	/
16 [38]	CdS nanowires	Pt	Pt-S_4	0.27–0.98 wt.%	impregnation	H_2	47.41 mmol g^{-1} h^{-1}	/
17 [140]	g-C_3N_4	Pt	Pt-C/Pt-N	0.17–1.7%	impregnation	H_2	34.2 mmol h^{-1}	/
18 [111]	MOF	Co	Co-N_2Cl_2O	3.3 wt.%	co-precipitation	H_2	27.853 mmol g^{-1}, 40 h	/
19 [141]	NG	Co	Co-N_2C	3.5 wt.% (Co-NG)	impregnation	H_2	677.44 umol g^{-1} h^{-1}	/
20 [122]	NG	Ni	Ni-N	0.26 wt.%	impregnation	H_2	1351.1 umol h^{-1}	48.2%, 420 nm
21 [100]	TiO2	(CH3)2Pt(COD)	O-Pt-O	/	impregnation	H_2	/	12%, 225–387 nm
22 [114]	TiO2	Cu, Co, Fe, Ni, Rh	Cu-O	0.75 wt.%	impregnation	H_2	16.6 mmol g^{-1} h^{-1}	45.5%, 340 nm
23 [42]	GaS nanosheet	Ru(IV)	Ru_1-S_6	2.4 wt.%	impregnation	H_2, O_2	340 umol g^{-1} h^{-1}	/
24 [97]	MOF−808-EDTA	Pt	Pt-N_2O_2	0.98 wt.%	impregnation	H_2	68.33 mmol g^{-1} h^{-1}	67.6%, 420 nm
25 [101]	g-C_3N_4	Pd	Pd-N	0.1 wt.%	impregnation	H_2	728 umol g^{-1} h^{-1}	/

Table 1. *Cont.*

	Supports	Single Atoms	Coordination	Loaded Content	Synthesis Methods	Products	Production Rate	AQE
26 [83]	CdS@CDs	Pt	Pt-S	1.15%	impregnation	H_2	45.5 mmol g^{-1} h^{-1}	29.8%, 400 nm
27 [142]	zeolitic imidazole framework	Co	/	0.57%	co-precipitation	H_2	6420 umol g^{-1} h^{-1}	/
28 [107]	g-C_3N_4	Pt, Au	Pt-N, Au-N	0.6 Pt, 0.8 (Au), wt.%	impregnation	H_2, O_2	H_2: 285 umol g^{-1} h^{-1}, H_2:O_2 = 2:1	/
29 [77]	N doped CDs	Co	Co-N4	3.27 wt.%	co-precipitation	O_2	245 umol g^{-1}, 4 h	/
30 [55]	g-C_3N_4	Au	Au-O	0.18 wt.%	impregnation	H_2	789.1 nmol h^{-1}	/
31 [117]	g-C_3N_4	Fe	Pt-N (DFT)	0.5 at.%	impregnation	H_2	3390 umol g^{-1} h^{-1}	6.89%, 420 nm
32 [129]	g-C_3N_4	Pt	Pt-N/O/Cl	0.35 mg m^{-2}	photo-deposition	H_2	174.5 mmol g^{-1} h^{-1}	0.544%, 420 nm
33 [66]	MOF	Pt	Pt-N	12 wt.%	co-precipitation	H_2	11320 umol g^{-1} h^{-1}	/
34 [143]	TiO_2	Pt	Pt-O	0.36 wt.%	photo-deposition	H_2	1077 umol h^{-1}	21.7%, 365 nm
35 [94]	defective TiO2	Pt	Pt-O	0.02wt%	impregnation	H_2	4458 umol g^{-1} h^{-1}	/
36 [103]	g-C_3N_4	Rh	Rh-P	/	impregnation	H_2	166.28 umol, 4 h	/
37 [105]	g-C_3N_4	Co	Co-P	0.13 wt.%	impregnation	O_2, H_2O_2	O_2: 15.5 umol, 4 h;	/
38 [88]	TiO2	Pt	/	0.03–0.47 at.%.	impregnation	H_2	/	/
39 [144]	g-C_3N_4	Ag	Ag-C_2N_2	3.7 wt.%	co-precipitation	H_2	1.8 mmol g^{-1} h^{-1}	/
40 [116]	g-C_3N_4	Ni	Ni-C/N	0.5 at%	impregnation	H_2	354.9 umol g^{-1} h^{-1}	/
41 [74]	N-doped CDs	Pt	Pt-C	0.2 wt.%	photo-deposition	H_2	175.3 umol h^{-1} cm^{-1}	/
42 [124]	$Zn_{0.25}Cd_{0.75}S$ QDs	Ni	Ni-S	0.15-0.125 at%	co-precipitation	H_2	18.87 mmol g^{-1} h^{-1}	/
43 [123]	coordination polymers	Cu	Cu-N	/	co-precipitation	H_2	57.64 mmol g^{-1} h^{-1}	/
44 [136]	g-C_3N_4	Pt	Pt-N	8.7 wt.%	ion exchange	H_2	22650 umol g^{-1} h^{-1}	22.5%, 420 nm
45 [39]	CdS	Ni	Ni-O	2.85 wt.%	photo-deposition	H_2	630.1 mmol g^{-1} h^{-1}	/
46 [145]	TiO_2 spheres	Ru	Ru-O	0.93 wt.%	impregnation	H_2	7.2 mmol g^{-1} h^{-1}	/
47 [99]	g-C_3N_4	Pt	Pt-N	/	impregnation	H_2	14.7 mmol g^{-1} h^{-1}	38.8%,435 nm
48 [106]	CdS	Pt	Pt-S	0.50 wt.%	impregnation	H_2	24.17 mmol g^{-1} h^{-1}	46%, 420 nm
49 [146]	TiO_2 nanosheet	Co	Co-O	1.11 wt.%	impregnation	H_2	1.682 mmol g^{-1} h^{-1}	/
50 [93]	g-C_3N_4	Pt	Pt-C4	1 wt.%	Photo-deposition	H_2	25.4 umol h^{-1}	0.5%, AM 1.5 illumination
51 [45]	Cs_2SnI_6	Pt	Pt-I_3	0.12 wt.%	impregnation	H_2	430 umol g^{-1} h^{-1}	/
52 [147]	unimolecular micelles	Pt	Pt-N, Pt-C-N	4.1 wt.%	co-precipitation	H_2	49465 umol g_{Pt}^{-1} h^{-1}	/

5. Summary and Prospect

SAPCs provide a new pathway for the construction of high performance cocatalyst/photocatalyst composites. For the past few years, the preparation method, characterization technology, theoretical modeling, and mechanism investigation of SAPCs have been developed rapidly, promoting the rational design and fabrication of more efficient SAPCs. As discussed above, benefitting from their low-coordination status, unique electric structures, and metal-support interactions, SAPCs can bring about unique advantages in comparison with the nanocluster-based, nanoparticle-based, and bulk catalysts. These include: (1) reduced usage amounts of metals (especially pertinent to noble metals) due to the ultrahigh atomic utilization; (2) distinguished catalytic activity, selectivity, and stability; and (3) simple model of the material system, facilitating the study of catalytic mechanism and photocatalyst design. Hence, SAPCs possess great potentials and good application prospects for photocatalytic water splitting.

Although SAPCs have shown excellent performance in photocatalysis, there remain several great challenges. The high surface free energy of isolated atoms makes it is intrinsically difficult to synthesize SAPCs, in consideration of the serious tendency for agglomeration of single atoms and the resultant deactivation during reaction. Further research should be undertaken to expand the library of supports, develop new synthesis methods, and improve the loading content and stability of single metal atoms. The newly supports such as BiOCl, perovskite, et al., provide more abundant coordination atoms different from the traditional N, O, C etc., which will bring new possibilities. Various synthesis methods, such as ion exchange, could be tried to synthesize SAPCs; Besides, the current studies exploiting single-atom photocatalysts for photocatalytic H_2 evolution mainly relied on the usage of sacrificial reagents. The design and creation of SAPCs capable of driving photocatalytic overall water splitting need to be further explored. Loading dual single metal atoms as bifunctional cocatalysts may be a promising strategy worthy to be investigated for improving the quantum efficiency of photocatalysis; Moreover, in-depth study of structure-function relationship and photocatalytic mechanism in SAPCs are strongly required, which require the exploration of advanced characterization techniques for precisely determining the single atoms. By making progress in these directions, it is believed that we can rationally construct SAPCs with optimized catalytic properties to realize practical application in solar energy conversion in the feature.

Author Contributions: J.Z. and J.L. proposed and guided this project. S.Z. contributed to the writing of this review article. B.B. revised this manuscript. All authors have read and agreed to the published version of the manuscript.

Funding: This research was funded by the National Natural Science Foundation of China (grant number 52072035, 51872030, 51631001, 51702016, 51902023, 21801015), Joint R&D Plan of Hongkong, Macao, Taiwan and Beijing (Z191100001619002), the Fundamental Research Funds for the Central Universities 2017CX01003 and the Beijing Institute of Technology Research Fund Program for Young Scholars.

Data Availability Statement: Data is contained within the article.

Conflicts of Interest: The authors declare no conflict of interest.

References

1. Fujishima, A.; Honda, K. Electrochemical Photolysis of Water at a Semiconductor Electrode. *Nature* **1972**, *238*, 37–38. [CrossRef]
2. Fu, C.F.; Wu, X.; Yang, J. Material Design for Photocatalytic Water Splitting from a Theoretical Perspective. *Adv. Mater.* **2018**, *30*, e1802106. [CrossRef]
3. Jafari, T.; Moharreri, E.; Amin, A.S.; Miao, R.; Song, W.; Suib, S.L. Photocatalytic Water Splitting-The Untamed Dream: A Review of Recent Advances. *Molecules* **2016**, *21*, 900. [CrossRef]
4. Tong, H.; Ouyang, S.; Bi, Y.; Umezawa, N.; Oshikiri, M.; Ye, J. Nano-Photocatalytic Materials: Possibilities and Challenges. *Adv. Mater.* **2012**, *24*, 229–251. [CrossRef]

5. Chen, X.; Shen, S.; Guo, L.; Mao, S.S. Semiconductor-Based Photocatalytic Hydrogen Generation. *Chem. Rev.* **2010**, *110*, 6503–6570. [CrossRef]
6. Maeda, K.; Domen, K. Photocatalytic Water Splitting: Recent Progress and Future Challenges. *J. Phys. Chem. Lett.* **2010**, *1*, 2655–2661. [CrossRef]
7. Wang, Q.; Domen, K. Particulate Photocatalysts for Light-Driven Water Splitting: Mechanisms, Challenges, and Design Strategies. *Chem. Rev.* **2020**, *120*, 919–985. [CrossRef] [PubMed]
8. Bai, S.; Zhang, N.; Gao, C.; Xiong, Y. Defect Engineering in Photocatalytic Materials. *Nano Energy* **2018**, *53*, 296–336. [CrossRef]
9. Wachs, I.E.; Phivilay, S.P.; Roberts, C.A. Reporting of Reactivity for Heterogeneous Photocatalysis. *ACS Catal.* **2013**, *3*, 2606–2611. [CrossRef]
10. Sultan, S.; Tiwari, J.N.; Singh, A.N.; Zhumagali, S.; Ha, M.; Myung, C.W.; Thangavel, P.; Kim, K.S. Single Atoms and Clusters Based Nanomaterials for Hydrogen Evolution, Oxygen Evolution Reactions, and Full Water Splitting. *Adv. Energy Mater.* **2019**, *9*, 1900624. [CrossRef]
11. Mitchell, S.; Perez-Ramirez, J. Single Atom Catalysis: A Decade of Stunning Progress and the Promise for a Bright Future. *Nat. Commun.* **2020**, *11*, 4302. [CrossRef] [PubMed]
12. Wei, X.; Wang, K.-X.; Guo, X.-X.; Chen, J.-S. Single-Site Photocatalysts with a Porous Structure. *Proc. R. Soc. A Math. Phys. Eng. Sci.* **2012**, *468*, 2099–2112. [CrossRef]
13. Yang, X.F.; Wang, A.; Qiao, B.; Li, J.; Liu, J.; Zhang, T. Single-Atom Catalysts: A New Frontier in Heterogeneous Catalysis. *Acc. Chem. Res.* **2013**, *46*, 1740–1748. [CrossRef] [PubMed]
14. Wang, B.; Cai, H.; Shen, S. Single Metal Atom Photocatalysis. *Small Methods* **2019**, *3*, 1800447. [CrossRef]
15. Zhu, Y.; Sokolowski, J.; Song, X.; He, Y.; Mei, Y.; Wu, G. Engineering Local Coordination Environments of Atomically Dispersed and Heteroatom-Coordinated Single Metal Site Electrocatalysts for Clean Energy-Conversion. *Adv. Energy Mater.* **2019**, *10*, 1902844. [CrossRef]
16. Wang, Q.; Zhang, D.; Chen, Y.; Fu, W.-F.; Lv, X.-J. Single-Atom Catalysts for Photocatalytic Reactions. *ACS Sustain. Chem. Eng.* **2019**, *7*, 6430–6443. [CrossRef]
17. Zhang, Y.; Xia, B.; Ran, J.; Davey, K.; Qiao, S.Z. Atomic-Level Reactive Sites for Semiconductor-Based Photocatalytic CO_2 Reduction. *Adv. Energy Mater.* **2020**, *10*, 1903879. [CrossRef]
18. Zhang, Q.; Guan, J. Recent Progress in Single-Atom Catalysts for Photocatalytic Water Splitting. *Sol. RRL* **2020**, *4*, 2000283. [CrossRef]
19. Zeng, L.; Xue, C. Single Metal Atom Decorated Photocatalysts: Progress and Challenges. *Nano Res.* **2020**, *14*, 934–944. [CrossRef]
20. Gao, C.; Low, J.; Long, R.; Kong, T.; Zhu, J.; Xiong, Y. Heterogeneous Single-Atom Photocatalysts: Fundamentals and Applications. *Chem. Rev.* **2020**, *120*, 12175–12216. [CrossRef]
21. Ji, S.; Qu, Y.; Wang, T.; Chen, Y.; Wang, G.; Li, X.; Dong, J.; Chen, Q.; Zhang, W.; Zhang, Z.; et al. Rare-Earth Single Erbium Atoms for Enhanced Photocatalytic CO_2 Reduction. *Angew. Chem. Int. Ed. Engl.* **2020**, *59*, 10651–10657. [CrossRef]
22. Sui, Y.; Liu, S.; Li, T.; Liu, Q.; Jiang, T.; Guo, Y.; Luo, J.-L. Atomically Dispersed Pt on Specific TiO_2 Facets for Photocatalytic H_2 Evolution. *J. Catal.* **2017**, *353*, 250–255. [CrossRef]
23. Wang, F.; Di Valentin, C.; Pacchioni, G. Doping of WO3 for Photocatalytic Water Splitting: Hints from Density Functional Theory. *J. Phys. Chem. C* **2012**, *116*, 8901–8909. [CrossRef]
24. Wang, J.; Xia, T.; Wang, L.; Zheng, X.; Qi, Z.; Gao, C.; Zhu, J.; Li, Z.; Xu, H.; Xiong, Y. Enabling Visible-Light-Driven Selective CO_2 Reduction by Doping Quantum Dots: Trapping Electrons and Suppressing H_2 Evolution. *Angew. Chem. Int. Ed. Engl.* **2018**, *57*, 16447–16451. [CrossRef]
25. Xiong, X.; Mao, C.; Yang, Z.; Zhang, Q.; Waterhouse, G.I.N.; Gu, L.; Zhang, T. Photocatalytic CO_2 Reduction to CO over Ni Single Atoms Supported on Defect-Rich Zirconia. *Adv. Energy Mater.* **2020**, *10*, 2002928. [CrossRef]
26. Takata, T.; Jiang, J.; Sakata, Y.; Nakabayashi, M.; Shibata, N.; Nandal, V.; Seki, K.; Hisatomi, T.; Domen, K. Photocatalytic Water Splitting with a Quantum Efficiency of Almost Unity. *Nature* **2020**, *581*, 411–414. [CrossRef]
27. Dong, S.; Li, B.; Cui, X.; Tan, S.; Wang, B. Photoresponses of Supported Au Single Atoms on TiO2(110) through the Metal-Induced Gap States. *J. Phys. Chem. Lett.* **2019**, *10*, 4683–4691. [CrossRef] [PubMed]
28. Fujiwara, K.; Pratsinis, S.E. Single Pd Atoms on TiO_2 Dominate Photocatalytic NOx Removal. *Appl. Catal. B* **2018**, *226*, 127–134. [CrossRef]
29. Jin, C.; Dai, Y.; Wei, W.; Ma, X.; Li, M.; Huang, B. Effects of Single Metal Atom (Pt, Pd, Rh and Ru) Adsorption on the Photocatalytic Properties of Anatase TiO_2. *Appl. Surf. Sci.* **2017**, *426*, 639–646. [CrossRef]
30. Linsebigler, A.L.; Lu, G.; Yates, J.T. Photocatalysis on TiO_2 Surfaces: Principles, Mechanisms, and Selected Results. *Chem. Rev.* **2002**, *95*, 735–758. [CrossRef]
31. Liu, S.; Wang, Y.; Wang, S.; You, M.; Hong, S.; Wu, T.-S.; Soo, Y.-L.; Zhao, Z.; Jiang, G.; Jieshan, Q.; et al. Photocatalytic Fixation of Nitrogen to Ammonia by Single Ru Atom Decorated TiO_2 Nanosheets. *ACS Sustain. Chem. Eng.* **2019**, *7*, 6813–6820. [CrossRef]
32. Xu, T.; Zhao, H.; Zheng, H.; Zhang, P. Atomically Pt Implanted Nanoporous TiO_2 Film for Photocatalytic Degradation of Trace Organic Pollutants in Water. *Chem. Eng. J.* **2020**, *385*, 123832. [CrossRef]
33. Xu, T.; Zheng, H.; Zhang, P. Isolated Pt Single Atomic Sites Anchored on Nanoporous TiO_2 Film for Highly Efficient Photocatalytic Degradation of Low Concentration Toluene. *J. Hazard. Mater.* **2020**, *388*, 121746. [CrossRef] [PubMed]

34. Trofimovaite, R.; Parlett, C.M.A.; Kumar, S.; Frattini, L.; Isaacs, M.A.; Wilson, K.; Olivi, L.; Coulson, B.; Debgupta, J.; Douthwaite, R.E.; et al. Single Atom Cu(I) Promoted Mesoporous Titanias for Photocatalytic Methyl Orange Depollution and H_2 Production. *Appl. Catal. B* **2018**, *232*, 501–511. [CrossRef]
35. Tao, J.; Luttrell, T.; Batzill, M. A Two-Dimensional Phase of TiO(2) with a Reduced Bandgap. *Nat. Chem.* **2011**, *3*, 296–300. [CrossRef]
36. Ida, S.; Kim, N.; Ertekin, E.; Takenaka, S.; Ishihara, T. Photocatalytic Reaction Centers in Two-Dimensional Titanium Oxide Crystals. *J. Am. Chem. Soc.* **2015**, *137*, 239–244. [CrossRef]
37. Nebel, R.; Macounová, K.M.; Tarábková, H.; Kavan, L.; Krtil, P. Selectivity of Photoelectrochemical Water Splitting on TiO_2 Anatase Single Crystals. *J. Phys. Chem. C* **2019**, *123*, 10857–10867. [CrossRef]
38. Zhou, P.; Zhang, Q.; Chao, Y.; Wang, L.; Li, Y.; Chen, H.; Gu, L.; Guo, S. Partially Reduced Pd Single Atoms on CdS Nanorods Enable Photocatalytic Reforming of Ethanol into High Value-Added Multicarbon Compound. *Chem* **2021**, *7*, 1033–1049. [CrossRef]
39. Zhang, J.; Xu, X.; Yang, L.; Cheng, D.; Cao, D. Single-Atom Ru Doping Induced Phase Transition of MoS_2 and S Vacancy for Hydrogen Evolution Reaction. *Small Methods* **2019**, *3*, 1900653. [CrossRef]
40. Li, G.; Duan, H.; Cheng, W.; Wang, C.; Hu, W.; Sun, Z.; Tan, H.; Li, N.; Ji, Q.; Wang, Y.; et al. Interlayer Photoelectron Transfer Boosted by Bridged Ru(IV) Atoms in GaS Nanosheets for Efficient Water Splitting. *ACS Appl. Mater. Interfaces* **2019**, *11*, 45561–45567. [CrossRef]
41. Gupta, S.S.; van Huis, M.A. Intermetallic Differences at CdS-Metal (Ni, Pd, Pt, and Au) Interfaces: From Single-Atom to Subnanometer Metal Clusters. *J. Phys. Chem. C Nanomater Interfaces* **2019**, *123*, 9298–9310. [CrossRef]
42. Wu, X.; Zhang, H.; Dong, J.; Qiu, M.; Kong, J.; Zhang, Y.; Li, Y.; Xu, G.; Zhang, J.; Ye, J. Surface Step Decoration of Isolated Atom as Electron Pumping: Atomic-Level Insights into Visible-Light Hydrogen Evolution. *Nano Energy* **2018**, *45*, 109–117. [CrossRef]
43. Zhang, H.; Dong, Y.; Zhao, S.; Wang, G.; Jiang, P.; Zhong, J.; Zhu, Y. Photochemical Preparation of Atomically Dispersed Nickel on Cadmium Sulfide for Superior Photocatalytic Hydogen Evolution. *Appl. Catal. B* **2020**, *261*, 118233. [CrossRef]
44. Shoji, S.; Peng, X.; Yamaguchi, A.; Watanabe, R.; Fukuhara, C.; Cho, Y.; Yamamoto, T.; Matsumura, S.; Yu, M.-W.; Ishii, S.; et al. Photocatalytic Uphill Conversion of Natural Gas Beyond the Limitation of Thermal Reaction Systems. *Nat. Catal.* **2020**, *3*, 148–153. [CrossRef]
45. Zhou, P.; Chen, H.; Chao, Y.; Zhang, Q.; Zhang, W.; Lv, F.; Gu, L.; Zhao, Q.; Wang, N.; Wang, J.; et al. Single-Atom Pt-I3 Sites on All-Inorganic Cs_2SnI_6 Perovskite for Efficient Photocatalytic Hydrogen Production. *Nat. Commun.* **2021**, *12*, 4412. [CrossRef]
46. Di, J.; Chen, C.; Yang, S.Z.; Chen, S.; Duan, M.; Xiong, J.; Zhu, C.; Long, R.; Hao, W.; Chi, Z.; et al. Isolated Single Atom Cobalt in Bi_3O_4Br Atomic Layers to Trigger Efficient CO_2 Photoreduction. *Nat. Commun.* **2019**, *10*, 2840. [CrossRef]
47. Zhao, Z.; Sun, Y.; Dong, F. Graphitic Carbon Nitride Based Nanocomposites: A Review. *Nanoscale* **2015**, *7*, 15–37. [CrossRef]
48. Wen, J.; Xie, J.; Chen, X.; Li, X. A Review on g-C_3N_4 -Based Photocatalysts. *Appl. Surf. Sci.* **2017**, *391*, 72–123. [CrossRef]
49. Fu, J.; Yu, J.; Jiang, C.; Cheng, B. g-C_3N_4-Based Heterostructured Photocatalysts. *Adv. Energy Mater.* **2018**, *8*, 1701503. [CrossRef]
50. Wang, X.; Maeda, K.; Thomas, A.; Takanabe, K.; Xin, G.; Carlsson, J.M.; Domen, K.; Antonietti, M. A Metal-Free Polymeric Photocatalyst for Hydrogen Production from Water Under Visible Light. *Nat. Mater.* **2009**, *8*, 76–80. [CrossRef]
51. Chen, Z.; Mitchell, S.; Vorobyeva, E.; Leary, R.K.; Hauert, R.; Furnival, T.; Ramasse, Q.M.; Thomas, J.M.; Midgley, P.A.; Dontsova, D.; et al. Stabilization of Single Metal Atoms on Graphitic Carbon Nitride. *Adv. Funct. Mater.* **2017**, *27*, 1605785. [CrossRef]
52. Li, Y.; Kong, T.; Shen, S. Artificial Photosynthesis with Polymeric Carbon Nitride: When Meeting Metal Nanoparticles, Single Atoms, and Molecular Complexes. *Small* **2019**, *15*, e1900772. [CrossRef] [PubMed]
53. Gao, G.; Jiao, Y.; Waclawik, E.R.; Du, A. Single Atom (Pd/Pt) Supported on Graphitic Carbon Nitride as an Efficient Photocatalyst for Visible-Light Reduction of Carbon Dioxide. *J. Am. Chem. Soc.* **2016**, *138*, 6292–6297. [CrossRef] [PubMed]
54. Li, Y.; Wang, Z.; Xia, T.; Ju, H.; Zhang, K.; Long, R.; Xu, Q.; Wang, C.; Song, L.; Zhu, J.; et al. Implementing Metal-to-Ligand Charge Transfer in Organic Semiconductor for Improved Visible-Near-Infrared Photocatalysis. *Adv. Mater.* **2016**, *28*, 6959–6965. [CrossRef] [PubMed]
55. Zeng, L.; Dai, C.; Liu, B.; Xue, C. Oxygen-Assisted Stabilization of Single-Atom Au During Photocatalytic Hydrogen Evolution. *J. Mater. Chem. A* **2019**, *7*, 24217–24221. [CrossRef]
56. Liu, W.; Cao, L.; Cheng, W.; Cao, Y.; Liu, X.; Zhang, W.; Mou, X.; Jin, L.; Zheng, X.; Che, W.; et al. Single-Site Active Cobalt-Based Photocatalyst with a Long Carrier Lifetime for Spontaneous Overall Water Splitting. *Angew. Chem. Int. Ed. Engl.* **2017**, *56*, 9312–9317. [CrossRef] [PubMed]
57. Yang, Y.; Li, F.; Chen, J.; Fan, J.; Xiang, Q. Single Au Atoms Anchored on Amino-Group-Enriched Graphitic Carbon Nitride for Photocatalytic CO_2 Reduction. *ChemSusChem* **2020**, *13*, 1979–1985. [CrossRef]
58. Li, B.; Wen, H.M.; Cui, Y.; Zhou, W.; Qian, G.; Chen, B. Emerging Multifunctional Metal-Organic Framework Materials. *Adv. Mater.* **2016**, *28*, 8819–8860. [PubMed]
59. Dhakshinamoorthy, A.; Li, Z.; Garcia, H. Catalysis and Photocatalysis by Metal Organic Frameworks. *Chem. Soc. Rev.* **2018**, *47*, 8134–8172. [CrossRef]
60. Wang, C.; Xie, Z.; de Krafft, K.E.; Lin, W. Doping Metal-Organic Frameworks for Water Oxidation, Carbon Dioxide Reduction, and Organic Photocatalysis. *J. Am. Chem. Soc.* **2011**, *133*, 13445–13454. [CrossRef]
61. Liu, J.; Fan, Y.-Z.; Li, X.; Wei, Z.; Xu, Y.-W.; Zhang, L.; Su, C.-Y. A Porous Rhodium(III)-Porphyrin Metal-Organic Framework as an Efficient and Selective Photocatalyst for CO_2 Reduction. *Appl. Catal. B* **2018**, *231*, 173–181. [CrossRef]

62. Wang, X.-S.; Chen, C.-H.; Ichihara, F.; Oshikiri, M.; Liang, J.; Li, L.; Li, Y.; Song, H.; Wang, S.; Zhang, T.; et al. Integration of Adsorption and Photosensitivity Capabilities into a Cationic Multivariate Metal-Organic Framework for Enhanced Visible-Light Photoreduction Reaction. *Appl. Catal. B* **2019**, *253*, 323–330. [CrossRef]
63. Liu, M.; Mu, Y.-F.; Yao, S.; Guo, S.; Guo, X.-W.; Zhang, Z.-M.; Lu, T.-B. Photosensitizing Single-Site Metal−organic Framework Enabling Visible-Light-Driven CO_2 Reduction for Syngas Production. *Appl. Catal. B* **2019**, *245*, 496–501. [CrossRef]
64. Jiao, L.; Jiang, H.-L. Metal-Organic-Framework-Based Single-Atom Catalysts for Energy Applications. *Chem* **2019**, *5*, 786–804. [CrossRef]
65. Zhang, H.; Wei, J.; Dong, J.; Liu, G.; Shi, L.; An, P.; Zhao, G.; Kong, J.; Wang, X.; Meng, X.; et al. Efficient Visible-Light-Driven Carbon Dioxide Reduction by a Single-Atom Implanted Metal-Organic Framework. *Angew. Chem. Int. Ed. Engl.* **2016**, *55*, 14310–14314. [CrossRef]
66. Zuo, Q.; Liu, T.; Chen, C.; Ji, Y.; Gong, X.; Mai, Y.; Zhou, Y. Ultrathin Metal-Organic Framework Nanosheets with Ultrahigh Loading of Single Pt Atoms for Efficient Visible-Light-Driven Photocatalytic H_2 Evolution. *Angew. Chem. Int. Ed. Engl.* **2019**, *58*, 10198–10203. [CrossRef] [PubMed]
67. Zeng, Y.; Zou, R.; Zhao, Y. Covalent Organic Frameworks for CO_2 Capture. *Adv. Mater.* **2016**, *28*, 2855–2873. [CrossRef]
68. Li, J.; Liu, P.; Tang, Y.; Huang, H.; Cui, H.; Mei, D.; Zhong, C. Single-Atom Pt–N3 Sites on the Stable Covalent Triazine Framework Nanosheets for Photocatalytic N_2 Fixation. *ACS Catal.* **2020**, *10*, 2431–2442. [CrossRef]
69. Zhong, W.; Sa, R.; Li, L.; He, Y.; Li, L.; Bi, J.; Zhuang, Z.; Yu, Y.; Zou, Z. A Covalent Organic Framework Bearing Single Ni Sites as a Synergistic Photocatalyst for Selective Photoreduction of CO_2 to CO. *J. Am. Chem. Soc.* **2019**, *141*, 7615–7621. [CrossRef]
70. Li, X.; Yu, J.; Wageh, S.; Al-Ghamdi, A.A.; Xie, J. Graphene in Photocatalysis: A Review. *Small* **2016**, *12*, 6640–6696. [CrossRef]
71. Xiang, Q.; Yu, J.; Jaroniec, M. Graphene-Based Semiconductor Photocatalysts. *Chem. Soc. Rev.* **2012**, *41*, 782–796. [CrossRef]
72. Gawande, M.B.; Fornasiero, P.; Zbořil, R. Carbon-Based Single-Atom Catalysts for Advanced Applications. *ACS Catal.* **2020**, *10*, 2231–2259. [CrossRef]
73. Zhou, S.; Shang, L.; Zhao, Y.; Shi, R.; Waterhouse, G.I.N.; Huang, Y.C.; Zheng, L.; Zhang, T. Pd Single-Atom Catalysts on Nitrogen-Doped Graphene for the Highly Selective Photothermal Hydrogenation of Acetylene to Ethylene. *Adv. Mater.* **2019**, *31*, e1900509. [CrossRef] [PubMed]
74. Luo, H.; Liu, Y.; Dimitrov, S.D.; Steier, L.; Guo, S.; Li, X.; Feng, J.; Xie, F.; Fang, Y.; Sapelkin, A.; et al. Pt Single-Atoms Supported on Nitrogen-Doped Carbon Dots for Highly Efficient Photocatalytic Hydrogen Generation. *J. Mater. Chem. A* **2020**, *8*, 14690–14696. [CrossRef]
75. Gao, C.; Chen, S.; Wang, Y.; Wang, J.; Zheng, X.; Zhu, J.; Song, L.; Zhang, W.; Xiong, Y. Heterogeneous Single-Atom Catalyst for Visible-Light-Driven High-Turnover CO_2 Reduction: The Role of Electron Transfer. *Adv. Mater.* **2018**, *30*, e1704624. [CrossRef]
76. Zhao, Q.; Yao, W.; Huang, C.; Wu, Q.; Xu, Q. Effective and Durable Co Single Atomic Cocatalysts for Photocatalytic Hydrogen Production. *ACS Appl. Mater. Interfaces* **2017**, *9*, 42734–42741. [CrossRef]
77. Miao, X.; Qu, D.; Yang, D.; Nie, B.; Zhao, Y.; Fan, H.; Sun, Z. Synthesis of Carbon Dots with Multiple Color Emission by Controlled Graphitization and Surface Functionalization. *Adv. Mater.* **2018**, *30*, 1704740. [CrossRef]
78. Wang, Q.; Li, J.; Tu, X.; Liu, H.; Shu, M.; Si, R.; Ferguson, C.T.J.; Zhang, K.A.I.; Li, R. Single Atomically Anchored Cobalt on Carbon Quantum Dots as Efficient Photocatalysts for Visible Light-Promoted Oxidation Reactions. *Chem. Mater.* **2019**, *32*, 734–743. [CrossRef]
79. Wang, H.; Luo, Q.; Liu, W.; Lin, Y.; Guan, Q.; Zheng, X.; Pan, H.; Zhu, J.; Sun, Z.; Wei, S.; et al. Quasi Pd1Ni Single-Atom Surface Alloy Catalyst Enables Hydrogenation of Nitriles to Secondary Amines. *Nat. Commun.* **2019**, *10*, 4998. [CrossRef]
80. Marcinkowski, M.D.; Darby, M.T.; Liu, J.; Wimble, J.M.; Lucci, F.R.; Lee, S.; Michaelides, A.; Flytzani-Stephanopoulos, M.; Stamatakis, M.; Sykes, E.C.H. Pt/Cu Single-Atom Alloys as Coke-Resistant Catalysts for Efficient C-H Activation. *Nat. Chem.* **2018**, *10*, 325–332. [CrossRef]
81. Liu, Z.; Hou, W.; Pavaskar, P.; Aykol, M.; Cronin, S.B. Plasmon Resonant Enhancement of Photocatalytic Water Splitting under Visible Illumination. *Nano Lett.* **2011**, *11*, 1111–1116. [CrossRef] [PubMed]
82. Zhou, L.; Martirez, J.M.P.; Finzel, J.; Zhang, C.; Swearer, D.F.; Tian, S.; Robatjazi, H.; Lou, M.; Dong, L.; Henderson, L.; et al. Light-Driven Methane Dry Reforming with Single Atomic Site Antenna-Reactor Plasmonic Photocatalysts. *Nat. Energy* **2020**, *5*, 61–70. [CrossRef]
83. Qiu, S.; Shen, Y.; Wei, G.; Yao, S.; Xi, W.; Shu, M.; Si, R.; Zhang, M.; Zhu, J.; An, C. Carbon Dots Decorated Ultrathin CdS Nanosheets Enabling In-Situ Anchored Pt Single Atoms: A Highly Efficient Solar-Driven Photocatalyst for Hydrogen Evolution. *Appl. Catal. B* **2019**, *259*, 118036. [CrossRef]
84. Wang, Y.; Wang, Y.; Xu, R. Photochemical Deposition of Pt on CdS for H_2 Evolution from Water: Markedly Enhanced Activity by Controlling Pt Reduction Environment. *J. Phys. Chem. C* **2013**, *117*, 783–790. [CrossRef]
85. Tong, T.; Zhu, B.; Jiang, C.; Cheng, B.; Yu, J. Mechanistic Insight into the Enhanced Photocatalytic Activity of Single-Atom Pt, Pd or Au-Embedded g-C_3N_4. *Appl. Surf. Sci.* **2018**, *433*, 1175–1183. [CrossRef]
86. Ran, J.; Zhang, J.; Yu, J.; Jaroniec, M.; Qiao, S.Z. Earth-Abundant Cocatalysts for Semiconductor-Based Photocatalytic Water Splitting. *Chem. Soc. Rev.* **2014**, *43*, 7787–7812. [CrossRef] [PubMed]
87. Zhu, Y.; Wang, T.; Xu, T.; Li, Y.; Wang, C. Size Effect of Pt Co-Catalyst on Photocatalytic Efficiency of g-C_3N_4 for Hydrogen Evolution. *Appl. Surf. Sci.* **2019**, *464*, 36–42. [CrossRef]

88. Hejazi, S.; Mohajernia, S.; Osuagwu, B.; Zoppellaro, G.; Andryskova, P.; Tomanec, O.; Kment, S.; Zboril, R.; Schmuki, P. On the Controlled Loading of Single Platinum Atoms as a Co-Catalyst on TiO_2 Anatase for Optimized Photocatalytic H_2 Generation. *Adv. Mater.* **2020**, *32*, e1908505. [CrossRef]
89. Tsao, C.; Fang, M.; Hsu, Y. Modulation of Interfacial Charge Dynamics of Semiconductor Heterostructures for Advanced Photocatalytic Applications. *Coord. Chem. Rev.* **2021**, *438*, 213876. [CrossRef]
90. Lai, T.-H.; Katsumata, K.-I.; Hsu, Y.-J. In Situ Charge Carrier Dynamics of Semiconductor Nanostructures for Advanced Photoelectrochemical and Photocatalytic Applications. *Nanophotonics* **2020**, *10*, 777–795. [CrossRef]
91. Chen, F.; Ma, T.; Zhang, T.; Zhang, Y.; Huang, H. Atomic-Level Charge Separation Strategies in Semiconductor-Based Photocatalysts. *Adv Mater.* **2021**, *33*, e2005256. [CrossRef]
92. Liu, L.; Corma, A. Metal Catalysts for Heterogeneous Catalysis: From Single Atoms to Nanoclusters and Nanoparticles. *Chem. Rev.* **2018**, *118*, 4981–5079. [CrossRef]
93. Yan, J.; Ji, Y.; Batmunkh, M.; An, P.; Zhang, J.; Fu, Y.; Jia, B.; Li, Y.; Liu, S.; Ye, J.; et al. Breaking Platinum Nanoparticles to Single-Atomic Pt-C_4 Co-catalysts for Enhanced Solar-to-Hydrogen Conversion. *Angew. Chem. Int. Ed. Engl.* **2021**, *60*, 2541–2547. [CrossRef] [PubMed]
94. Chen, Y.; Ji, S.; Sun, W.; Lei, Y.; Wang, Q.; Li, A.; Chen, W.; Zhou, G.; Zhang, Z.; Wang, Y.; et al. Engineering the Atomic Interface with Single Platinum Atoms for Enhanced Photocatalytic Hydrogen Production. *Angew. Chem. Int. Ed. Engl.* **2020**, *59*, 1295–1301. [CrossRef]
95. Fang, X.; Shang, Q.; Wang, Y.; Jiao, L.; Yao, T.; Li, Y.; Zhang, Q.; Luo, Y.; Jiang, H.L. Single Pt Atoms Confined into a Metal-Organic Framework for Efficient Photocatalysis. *Adv. Mater.* **2018**, *30*, 1705112. [CrossRef]
96. Ou, M.; Wan, S.; Zhong, Q.; Zhang, S.; Wang, Y. Single Pt Atoms Deposition on g-C_3N_4 Nanosheets for Photocatalytic H_2 Evolution or NO Oxidation under Visible Light. *Int. J. Hydrogen Energy* **2017**, *42*, 27043–27054. [CrossRef]
97. Li, J.; Huang, H.; Liu, P.; Song, X.; Mei, D.; Tang, Y.; Wang, X.; Zhong, C. Metal-Organic Framework Encapsulated Single-Atom Pt Catalysts for Efficient Photocatalytic Hydrogen Evolution. *J. Catal.* **2019**, *375*, 351–360. [CrossRef]
98. Li, X.; Bi, W.; Zhang, L.; Tao, S.; Chu, W.; Zhang, Q.; Luo, Y.; Wu, C.; Xie, Y. Single-Atom Pt as Co-Catalyst for Enhanced Photocatalytic H_2 Evolution. *Adv. Mater.* **2016**, *28*, 2427–2431. [CrossRef] [PubMed]
99. Zhang, L.; Long, R.; Zhang, Y.; Duan, D.; Xiong, Y.; Zhang, Y.; Bi, Y. Direct Observation of Dynamic Bond Evolution in Single-Atom Pt/C_3N_4 Catalysts. *Angew. Chem. Int. Ed. Engl.* **2020**, *59*, 6224–6229. [CrossRef]
100. Jeantelot, G.; Qureshi, M.; Harb, M.; Ould-Chikh, S.; Anjum, D.H.; Abou-Hamad, E.; Aguilar-Tapia, A.; Hazemann, J.L.; Takanabe, K.; Basset, J.M. TiO_2-Supported Pt Single Atoms by Surface Organometallic Chemistry for Photocatalytic Hydrogen Evolution. *Phys. Chem. Chem. Phys.* **2019**, *21*, 24429–24440. [CrossRef]
101. Liu, L.; Wu, X.; Wang, L.; Xu, X.; Gan, L.; Si, Z.; Li, J.; Zhang, Q.; Liu, Y.; Zhao, Y.; et al. Atomic Palladium on Graphitic Carbon Nitride as a Hydrogen Evolution Catalyst under Visible Light Irradiation. *Comm. Chem.* **2019**, *2*, 1–8. [CrossRef]
102. Nie, G.; Li, P.; Liang, J.-X.; Zhu, C. Theoretical Investigation on the Photocatalytic Activity of the Au/g-C_3N_4 Monolayer. *J. Theor. Comput. Chem.* **2017**, *16*, 1750013. [CrossRef]
103. Chen, Z.; Bu, Y.; Wang, L.; Wang, X.; Ao, J.-P. Single-Sites Rh-Phosphide Modified Carbon Nitride Photocatalyst for Boosting Hydrogen Evolution under Visible Light. *Appl. Catal. B* **2020**, *274*, 119117. [CrossRef]
104. Cao, S.; Li, H.; Tong, T.; Chen, H.-C.; Yu, A.; Yu, J.; Chen, H.M. Single-Atom Engineering of Directional Charge Transfer Channels and Active Sites for Photocatalytic Hydrogen Evolution. *Adv. Funct. Mater.* **2018**, *28*, 1802169. [CrossRef]
105. Chu, C.; Zhu, Q.; Pan, Z.; Gupta, S.; Huang, D.; Du, Y.; Weon, S.; Wu, Y.; Muhich, C.; Stavitski, E.; et al. Spatially Separating Redox Centers on 2D Carbon Nitride with Cobalt Single Atom for Photocatalytic H_2O_2 Production. *Pans* **2020**, *117*, 6376–6382. [CrossRef] [PubMed]
106. Feng, R.; Wan, K.; Sui, X.; Zhao, N.; Li, H.; Lei, W.; Yu, J.; Liu, X.; Shi, X.; Zhai, M.; et al. Anchoring Single Pt Atoms and Black Phosphorene Dual Co-Catalysts on CdS Nanospheres to Boost Visible-Light Photocatalytic H_2 Evolution. *Nano Today* **2021**, *37*, 101080. [CrossRef]
107. Su, H.; Liu, M.; Cheng, W.; Zhao, X.; Hu, F.; Liu, Q. Heterogeneous Single-Site Synergetic Catalysis for Spontaneous Photocatalytic Overall Water Splitting. *J. Mater. Chem. A* **2019**, *7*, 11170–11176. [CrossRef]
108. Jiang, Z.; Sun, W.; Miao, W.; Yuan, Z.; Yang, G.; Kong, F.; Yan, T.; Chen, J.; Huang, B.; An, C.; et al. Living Atomically Dispersed Cu Ultrathin TiO_2 Nanosheet CO_2 Reduction Photocatalyst. *Adv. Sci.* **2019**, *6*, 1900289. [CrossRef]
109. Zhao, J.; Chen, Z. Single Mo Atom Supported on Defective Boron Nitride Monolayer as an Efficient Electrocatalyst for Nitrogen Fixation: A Computational Study. *J. Am. Chem. Soc.* **2017**, *139*, 12480–12487. [CrossRef]
110. Neubert, S.; Mitoraj, D.; Shevlin, S.A.; Pulisova, P.; Heimann, M.; Du, Y.; Goh, G.K.L.; Pacia, M.; Kruczała, K.; Turner, S.; et al. Highly Efficient Rutile TiO_2 Photocatalysts with Single Cu(2) and Fe(3) Surface Catalytic Sites. *J. Mater. Chem. A* **2016**, *4*, 3127–3138. [CrossRef]
111. Cao, Y.; Chen, S.; Luo, Q.; Yan, H.; Lin, Y.; Liu, W.; Cao, L.; Lu, J.; Yang, J.; Yao, T.; et al. Atomic-Level Insight into Optimizing the Hydrogen Evolution Pathway over a Co_1-N_4 Single-Site Photocatalyst. *Angew. Chem. Int. Ed. Engl.* **2017**, *56*, 12191–12196. [CrossRef]
112. Yang, S.; Pattengale, B.; Lee, S.; Huang, J. Real-Time Visualization of Active Species in a Single-Site Metal-Organic Framework Photocatalyst. *ACS Energy Lett.* **2018**, *3*, 532–539. [CrossRef]

113. Huang, P.; Huang, J.; Pantovich, S.A.; Carl, A.D.; Fenton, T.G.; Caputo, C.A.; Grimm, R.L.; Frenkel, A.I.; Li, G. Selective CO_2 Reduction Catalyzed by Single Cobalt Sites on Carbon Nitride under Visible-Light Irradiation. *J. Am. Chem. Soc.* **2018**, *140*, 16042–16047. [CrossRef]
114. Lee, B.H.; Park, S.; Kim, M.; Sinha, A.K.; Lee, S.C.; Jung, E.; Chang, W.J.; Lee, K.S.; Kim, J.H.; Cho, S.P.; et al. Reversible and Cooperative Photoactivation of Single-Atom Cu/TiO_2 Photocatalysts. *Nat. Mater.* **2019**, *18*, 620–626. [CrossRef] [PubMed]
115. Wu, Z.-Y.; Ji, W.-B.; Hu, B.-C.; Liang, H.-W.; Xu, X.-X.; Yu, Z.-L.; Li, B.-Y.; Yu, S.-H. Partially Oxidized Ni Nanoparticles Supported on Ni-N Co-doped Carbon Nanofibers As Bifunctional Electrocatalysts for Overall Water Splitting. *Nano Energy* **2018**, *51*, 286–293. [CrossRef]
116. Jin, X.; Wang, R.; Zhang, L.; Si, R.; Shen, M.; Wang, M.; Tian, J.; Shi, J. Electron Configuration Modulation of Nickel Single Atoms for Elevated Photocatalytic Hydrogen Evolution. *Angew. Chem. Int. Ed. Engl.* **2020**, *59*, 6827–6831. [CrossRef] [PubMed]
117. Zhang, W.; Peng, Q.; Shi, L.; Yao, Q.; Wang, X.; Yu, A.; Chen, Z.; Fu, Y. Merging Single-Atom-Dispersed Iron and Graphitic Carbon Nitride to a Joint Electronic System for High-Efficiency Photocatalytic Hydrogen Evolution. *Small* **2019**, *15*, e1905166. [CrossRef] [PubMed]
118. Yang, H.; Shang, L.; Zhang, Q.; Shi, R.; Waterhouse, G.I.N.; Gu, L.; Zhang, T. A Universal Ligand Mediated Method for Large Scale Synthesis of Transition Metal Single Atom Catalysts. *Nat. Commun.* **2019**, *10*, 4585. [CrossRef]
119. Ji, S.; Chen, Y.; Wang, X.; Zhang, Z.; Wang, D.; Li, Y. Chemical Synthesis of Single Atomic Site Catalysts. *Chem. Rev.* **2020**, *120*, 11900–11955. [CrossRef]
120. Xia, T.; Long, R.; Gao, C.; Xiong, Y. Design of Atomically Dispersed Catalytic Sites for Photocatalytic CO_2 Reduction. *Nanoscale* **2019**, *11*, 11064–11070. [CrossRef]
121. He, T.; Chen, S.; Ni, B.; Gong, Y.; Wu, Z.; Song, L.; Gu, L.; Hu, W.; Wang, X. Zirconium-Porphyrin-Based Metal-Organic Framework Hollow Nanotubes for Immobilization of Noble-Metal Single Atoms. *Angew. Chem. Int. Ed. Engl.* **2018**, *57*, 3493–3498. [CrossRef] [PubMed]
122. Zhao, Q.; Sun, J.; Li, S.; Huang, C.; Yao, W.; Chen, W.; Zeng, T.; Wu, Q.; Xu, Q. Single Nickel Atoms Anchored on Nitrogen-Doped Graphene as a Highly Active Cocatalyst for Photocatalytic H_2 Evolution. *ACS Catal.* **2018**, *8*, 11863–11874. [CrossRef]
123. Zang, Y.; Zhang, J.; Wang, R.; Wang, Z.D.; Zhu, Y.; Ren, X.; Li, S.; Dong, X.Y.; Zang, S.Q. Inter-Chain Double-Site Synergistic Photocatalytic Hydrogen Evolution in Robust Cuprous Coordination Polymers. *Chem. Commun.* **2020**, *56*, 6261–6264. [CrossRef] [PubMed]
124. Su, D.W.; Ran, J.; Zhuang, Z.W.; Chen, C.; Qiao, S.Z.; Li, Y.D.; Wang, G.X. Atomically Dispersed Ni in Cadmium-Zinc Sulfide Quantum Dots for High-Performance Visible-Light Photocatalytic Hydrogen Production. *Sci. Adv.* **2020**, *6*, eaaz8447. [CrossRef]
125. Wang, F.; Wang, Y.; Li, Y.; Cui, X.; Zhang, Q.; Xie, Z.; Liu, H.; Feng, Y.; Lv, W.; Liu, G. The Facile Synthesis of a Single Atom-Dispersed Silver-Modified Ultrathin g-C_3N_4 Hybrid for the Enhanced Visible-Light Photocatalytic Degradation of Sulfamethazine With Peroxymonosulfate. *Dalton Trans.* **2018**, *47*, 6924–6933. [CrossRef] [PubMed]
126. Guo, X.-W.; Chen, S.-M.; Wang, H.-J.; Zhang, Z.-M.; Lin, H.; Song, L.; Lu, T.-B. Single-Atom Molybdenum Immobilized on Photoactive Carbon Nitride as Efficient Photocatalysts for Ambient Nitrogen Fixation in Pure Water. *J. Mater. Chem. A* **2019**, *7*, 19831–19837. [CrossRef]
127. Du, X.L.; Wang, X.L.; Li, Y.H.; Wang, Y.L.; Zhao, J.J.; Fang, L.J.; Zheng, L.R.; Tong, H.; Yang, H.G. Isolation of Single Pt Atoms in a Silver Cluster: Forming Highly Efficient Silver-Based Cocatalysts for Photocatalytic Hydrogen Evolution. *Chem. Commun.* **2017**, *53*, 9402–9405. [CrossRef] [PubMed]
128. Wenderich, K.; Mul, G. Methods, Mechanism, and Applications of Photodeposition in Photocatalysis: A Review. *Chem. Rev.* **2016**, *116*, 14587–14619. [CrossRef]
129. Zhou, P.; Lv, F.; Li, N.; Zhang, Y.; Mu, Z.; Tang, Y.; Lai, J.; Chao, Y.; Luo, M.; Lin, F.; et al. Strengthening Reactive Metal-Support Interaction to Stabilize High-Density Pt Single Atoms on Electron-Deficient g-C_3N_4 for Boosting Photocatalytic H_2 Production. *Nano Energy* **2019**, *56*, 127–137. [CrossRef]
130. Yu, H.; Cao, C.; Wang, X.; Yu, J. Ag-Modified BiOCl Single-Crystal Nanosheets: Dependence of Photocatalytic Performance on the Region-Selective Deposition of Ag Nanoparticles. *J. Phys. Chem. C* **2017**, *121*, 13191–13201. [CrossRef]
131. Meng, A.; Zhang, J.; Xu, D.; Cheng, B.; Yu, J. Enhanced Photocatalytic H_2 Production Activity of Anatase TiO_2 Nanosheet by Selectively Depositing Du-Al-Cocatalysts on {101} and {001} Facets. *Appl. Catal. B* **2016**, *198*, 286–294. [CrossRef]
132. Lu, J.; Elam, J.W.; Stair, P.C. Atomic Layer Deposition-Sequential Self-Limiting Surface Reactions for Advanced Catalyst "Bottom-Up" Synthesis. *Surf. Sci. Rep.* **2016**, *71*, 410–472. [CrossRef]
133. Shi, X.; Lin, Y.; Huang, L.; Sun, Z.; Yang, Y.; Zhou, X.; Vovk, E.; Liu, X.; Huang, X.; Sun, M.; et al. Copper Catalysts in Semihydrogenation of Acetylene: From Single Atoms to Nanoparticles. *ACS Catal.* **2020**, *10*, 3495–3504. [CrossRef]
134. Cheng, N.; Stambula, S.; Wang, D.; Banis, M.N.; Liu, J.; Riese, A.; Xiao, B.; Li, R.; Sham, T.K.; Liu, L.M.; et al. Platinum Single-Atom and Cluster Catalysis of the Hydrogen Evolution Reaction. *Nat. Commun.* **2016**, *7*, 13638. [CrossRef]
135. Wang, X.; Jin, B.; Jin, Y.; Wu, T.; Ma, L.; Liang, X. Supported Single Fe Atoms Prepared via Atomic Layer Deposition for Catalytic Reactions. *ACS Appl. Nano Mater.* **2020**, *3*, 2867–2874. [CrossRef]
136. Zeng, Z.; Su, Y.; Quan, X.; Choi, W.; Zhang, G.; Liu, N.; Kim, B.; Chen, S.; Yu, H.; Zhang, S. Single-Atom Platinum Confined by the Interlayer Nanospace of Carbon Nitride for Efficient Photocatalytic Hydrogen Evolution. *Nano Energy* **2020**, *69*, 104409. [CrossRef]

137. Cao, Y.; Wang, D.; Lin, Y.; Liu, W.; Cao, L.; Liu, X.; Zhang, W.; Mou, X.; Fang, S.; Shen, X.; et al. Single Pt Atom with Highly Vacant d-Orbital for Accelerating Photocatalytic H_2 Evolution. *ACS Appl. Energ. Mater.* **2018**, *1*, 6082–6088. [CrossRef]
138. Su, H.; Che, W.; Tang, F.; Cheng, W.; Zhao, X.; Zhang, H.; Liu, Q. Valence Band Engineering via PtII Single-Atom Confinement Realizing Photocatalytic Water Splitting. *J. Phys. Chem. C* **2018**, *122*, 21108–21114. [CrossRef]
139. Zhang, G.; Huang, C.; Wang, X. Dispersing Molecular Cobalt in Graphitic Carbon Nitride Frameworks for Photocatalytic Water Oxidation. *Small* **2015**, *11*, 1215–1221. [CrossRef]
140. Xue, Y.; Lei, Y.; Liu, X.; Li, Y.; Deng, W.; Wang, F.; Min, S. Highly Active Dye-Sensitized Photocatalytic H_2 Evolution Catalyzed by a Single-Atom Pt Cocatalyst Anchored Onto g-C_3N_4 Nanosheets under Long-Wavelength Visible Light Irradiation. *New, J. Chem.* **2018**, *42*, 14083–14086. [CrossRef]
141. Yi, L.; Lan, F.; Li, J.; Zhao, C. Efficient Noble-Metal-Free Co-NG/TiO_2 Photocatalyst for H_2 Evolution: Synergistic Effect between Single-Atom Co and N-Doped Graphene for Enhanced Photocatalytic Activity. *ACS Sustain. Chem. Eng.* **2018**, *6*, 12766–12775. [CrossRef]
142. Ran, J.; Zhang, H.; Qu, J.; Xia, B.; Zhang, X.; Chen, S.; Song, L.; Jing, L.; Zheng, R.; Qiao, S.Z. Atomically Dispersed Single Co Sites in Zeolitic Imidazole Frameworks Promoting High-Efficiency Visible-Light-Driven Hydrogen Production. *Chem.-Eur. J.* **2019**, *25*, 9670–9677. [CrossRef]
143. Cai, S.; Wang, L.; Heng, S.; Li, H.; Bai, Y.; Dang, D.; Wang, Q.; Zhang, P.; He, C. Interaction of Single-Atom Platinum–Oxygen Vacancy Defects for the Boosted Photosplitting Water H_2 Evolution and CO_2 Photoreduction: Experimental and Theoretical Study. *J. Phys. Chem. C* **2020**, *124*, 24566–24579. [CrossRef]
144. Jiang, X.H.; Zhang, L.S.; Liu, H.Y.; Wu, D.S.; Wu, F.Y.; Tian, L.; Liu, L.L.; Zou, J.P.; Luo, S.L.; Chen, B.B. Silver Single Atom in Carbon Nitride Catalyst for Highly Efficient Photocatalytic Hydrogen Evolution. *Angew. Chem. Int. Ed. Engl.* **2020**, *59*, 23112–23116. [CrossRef] [PubMed]
145. Zhang, H.; Zuo, S.; Qiu, M.; Wang, S.; Zhang, Y.; Zhang, J.; Lou, X.W.D. Direct Probing of Atomically Dispersed Ru Species Over Multi-Edged TiO_2 for Highly Efficient Photocatalytic Hydrogen Evolution. *Sci. Adv.* **2020**, *6*, eabb9823. [CrossRef]
146. Wu, X.; Zuo, S.; Qiu, M.; Li, Y.; Zhang, Y.; An, P.; Zhang, J.; Zhang, H.; Zhang, J. Atomically Defined Co on Two-Dimensional TiO_2 Nanosheet for Photocatalytic Hydrogen Evolution. *Chem. Eng. J.* **2021**, *420*, 127681. [CrossRef]
147. Zuo, Q.; Feng, K.; Zhong, J.; Mai, Y.; Zhou, Y. Single-Metal-Atom Polymeric Unimolecular Micelles for Switchable Photocatalytic H_2 Evolution. *CCS Chemistry* **2021**, *3*, 1963–1971. [CrossRef]